February 2019

Doctoral dissertation

Development of preventive and therapeutic materials for degenerative arthritis using *Anthriscus sylvestris* leaves aqueous extract

Graduate School of Chosun University

Department of Biodental Engineering

Seul Ah Lee

Development of preventive and therapeutic materials for degenerative arthritis using *Anthriscus sylvestris* leaves aqueous extract

전호잎 열수추출물을 이용한 퇴행성관절염 예방 및 치료 소재 개발

2019년 2월 25일

조선대학교 대학원

치의생명공학과

이 슬 아

Development of preventive and therapeutic materials for degenerative arthritis using *Anthriscus sylvestris* leaves aqueous extract

지도교수 김 춘 성

이 논문을 이학 박사학위 논문으로 제출함

2018년 10월

조선대학교 대학원

치의생명공학과

이 슬 아

이슬아의 박사학위 논문을 인준함

위원장 조 선 대 학 교 교 수 김 홍 중 (인)

위 원 숙명여자대학교 교 수 양 영 (인)

위 원 조 선 대 학 교 교 수 김 도 경 (인)

위 원 조 선 대 학 교 교 수 김 재 성 (인)

위 원 조 선 대 학 교 교 수 김 춘 성 (인)

2018년 12월

조선대학교 대학원

Contents

List of Figures

List of Table

Abbreviation

OA ····· Osteoarthritis
ROS ····· Reactive oxigen species
RNS ····· Reactive nigrogen species
IL-1β ····· Interleukin 1 beta
MMP ····· Matrix metalloproteinase
ADAMTS ····· A disintegrin and metalloprotease with thrombospondin motifs
NO ····· Nitrite oxide
PGE_2 ····· Prostaglandin E_2
COL2A1 ····· Collagen type II
ECM ····· Extracellular matrix
NSAIDs ····· Non-steroidal anti-inflammatory drugs
ACLT ····· Anterior cruciate ligament transection
AE-ASL ····· Aqueous extract of *Anthriscus sylvestirs*
DMEM ····· Dulbecco's modified Eagle's medium
DMEM/F12 ····· Dulbecco's modified Eagle's medium/Nutrient mixture F-12
FBS ····· Fetal bovine serum
LPS ····· Lipopolysaccharide
DMMB ····· Dimethylmethylene blue
MTT ····· 3-(4,5-dimethylthiazol-2-yl)-2,5-diphenyltetrazolium bromide
PBS ····· Phosphate buffered saline
DMSO ····· Dimethyl sulfoxide
RT-PCR ····· Reverse transcription-polymerase chain reaction
TBST ····· Tris-buffered saline containing 0.1% Tween 20
BCA ····· Bicinchoninic acid
SDS-PAGE ····· Sodium dodecyl sulfate–polyacrylamide gel electrophoresis
PVDF ····· Polyvinylidene difluoride
HRP ····· Horseradish peroxidase

ECL ····· Enhanced chemiluminescence
sGAG ····· Sulfated glycosaminoglycan
Hcl ····· Hydrochloric acid
MMTL ····· Medial meniscotibial ligament
DMM ····· Destabilization of the medial meniscus
TFA/DW ····· Trifluoroacetic acid/water
TFA/MeCN ····· Trifluoroacetic acid/acetonitrile
COX-2 ····· Cyclooxygenase 2
iNOS ····· Inducible nitric oxide synthase
TNF-α ····· Tumor necrosis factor alpha
IL-6 ····· Interleukin 6
ERK ····· Extracellular signal-regulated kinase
JNK ····· c-Jun N-terminal kinase
NF-κB ····· Nuclear factor kappa B
IκB-α ····· Inhibitor of kappa B alpha
MAPK ····· Mitogen-activated protein kinase

초 록

전호잎 열수추출물을 이용한 퇴행성관절염 예방 및 치료 소재 개발

이 슬 아
지도교수 : 김 춘 성
치의생명공학과
조선대학교 일반대학원

퇴행성관절염(osteoarthritis, OA)은 점진적이고 비가역적인 연골 마모에 의해 유도되는 대표적인 관절질환으로 65세 이상 사람들의 50% 이상이 앓고 있는 흔한 노인퇴행성질환이다. 퇴행성관절염은 연골마모와 골극(osteophyte)이 형성되는 것이 특징이며, 발병이 진행될수록 연골하골(subchondral bone)의 remodeling과 함께 신경이 침투하여 통증이 유도되고 궁극적으로 움직임에 불편함을 느끼게 된다. 분자학적인 관점에서 봤을 때, 퇴행성관절염은 oxidative와 nitrosative에 의한 스트레스, 염증 관련 인자들의 과발현에 의한 염증 과유도, 그리고 연골기질 분해효소 활성에 의한 연골기질 분해 등 다양한 원인 인자들이 있으나, 염증에 의한 연골기질 분해가 퇴행성관절염의 직접적인 주요 원인으로 알려져 있다. 염증은 염증관련 인자들(inducible nitrite oxide synthase(iNOS), cyclooxygenase(COX)-2, tumor necrosis factor(TNF)-α, interleukin(IL)-1β, IL-6 등)의 발현을 증가시키고 이들의 paracrine 및 autocrine 반응에 의해 염증환경을 지속적으로 유지시킨다. 또, 이러한 염증반응은 연골기질 분해효소(matrix metalloproteinase(MMP)s, a disintegrin and metalloproteinase with thrombospondin motifs(ADAMTS) family 등)의 활성을 증가시켜 연골기질을 분해시키며, 염증과 연골기질 분해효소 활성 증가

의 반복적인 악순환을 통해 퇴행성관절염의 진행을 가속화시킨다. 현재, 관절 통증을 완화시키거나 움직임을 향상시키는 등 퇴행성관절염의 증상 완화를 위해 약리학적으로는 비스테로이성 항염증제(non-steroidal anti-inflammatory drugs, NSAIDs)가 처방되거나 무릎관절 치환술과 같은 수술이 권고되고 있으나 처방되는 이러한 약들은 장기간 복용 시 퇴행성관절염 진행을 지연시키기거나 회복시키기보다는 위장 기능 약화와 신장 기능 약화와 같은 부작용을 초래한다. 따라서 퇴행성관절염을 예방하거나 진행을 지연시키고 증상을 완화시킬 수 있는 건강기능식품 혹은 약에 대한 개발 필요성이 대두되고 있으며, 최근에는 전통적인 약용식물에서 그 후보 물질을 찾으려는 노력이 증가하고 있다.

전호(*Anthriscus sylvestris* (L.) Hoffm.)는 산형과에 속하는 미나리과의 여러해살이풀로 유럽, 뉴질랜드와 한국 등의 산이나 들 전역에 넓게 분포해 있으며, 전호의 뿌리는 혈액순환을 좋게 하고 어혈을 풀어주며 열을 내리는 등의 효능으로 인해 예로부터 동양의학에서 다양한 질환의 치료제로 사용되어져 왔다. 전호는 많은 리그난 계열 성분과 폴리페놀 성분을 다량 함유하고 있으며, anthricin과 같은 리그난 계열은 암세포 성장 억제에 탁월한 효과가 있고, cynaroside과 chlorogenic acid과 같은 폴리페놀 성분은 항산화 효과가 있는 것으로 알려져 있다. 그러나 이외에 전호잎 열수추출물의 생리활성 연구는 보고되지 않았으며, 본 연구에서는 전호잎 열수추출물(aqueous extract of *Anthriscus sylvestris* leaves, AE-ASL)의 항염증 효과뿐만 아니라 이 효과를 기반으로 한 염증에 대한 연골보호효과를 평가하였다.

마우스 대식세포 RAW264.7과 랫트 초대배양 연골세포에 전호잎 열수추출물을 1시간 전처리한 후 각각 lipopolysaccharide(LPS, 0.2μg/mL)와 IL-1β (20ng/mL)를 24시간동안 처리하여 염증을 유도하였다. Nitrite의 생성량은 Griess reagent로 측정하였으며, prostaglandin E_2(PGE_2), aggrecan(ACAN)과 collagen type II(COL2A1)의 함량은 ELISA를 통해 측정하였다. iNOS, COX-2, TNF-α, IL-1β, IL-6, MMP-3와 MMP-13의 mRNA 발현 수준은 중합효소연쇄반응 기법을 통해 확인하였으며, iNOS, COX-2, TNF-α, IL-1β, IL-6, MMP-3, MMP-13, ADAMTS-4, mitogen-activated protein

kinases(MAPKs)과 nuclear factor-kappa(NF)-κB의 단백 발현은 웨스턴 블랏 기법을 통해 확인하였다. 또, 염증에 의해 분해되어 나온 황산 당아미노클리칸(sulfated glycosaminoglycan)의 함량은 DMMB assay를 통해 확인하였으며, 프로테오글리칸(proteoglycan)은 알시안 블루(alcian blue) 염색을 통해 확인하였다. 생체 내 연구를 위해 항염증 효능평가는 카라기난(carrageenan)에 의한 발 부종(paw edema) 실험동물 모델을 이용하였으며, 연골보호 효능평가는 반월판 불안정(destabilization of the medial meniscus, DMM)에 의한 퇴행성관절염 실험동물 모델에 전호잎 열수추출물을 8주 동안 매일 경구투여한 후 조직학적 검사를 수행하여 연골 파괴 및 프로테오글리칸의 손실 정도를 평가하여 그 효능을 분석하였다.

마우스 대식세포에서 전호잎 열수추출물의 전처리는 염증에 의해 증가된 nitrite와 PGE_2의 생성을 감소시켰으며, iNOS, COX-2, TNF-α, IL-1β와 IL-6의 mRNA 발현과 단백 발현 수준을 농도-의존적으로 감소시켰다. 그리고 전호잎 열수추출물은 염증에 의해 유도된 MAPKs(ERK, JNK, p38 MAPK)의 인산화를 억제하였으며, IkB-α의 인산화를 억제시킴으로써 NF-κB의 subunit인 p65의 핵으로의 이동을 억제하였다. 따라서 이러한 결과는 마우스 대식세포 RAW264.7에서 전호잎 열수추출물의 항염증 효과가 MAPKs와 NF-κB 신호전달체계에 의해 매개될 수 있음을 시사하고 있다. 카라기난에 의한 발 부종 실험에서 전호잎 열수추출물 50mg/kg, 100mg/kg, 그리고 200mg/kg을 경구투여 한 결과, 카라기난 주입 후 4시간 째에 카라기난만 주입된 군의 부종과 비교하였을 때, 50mg/kg 군에서 평균 15%, 100mg/kg에서 31%, 그리고 200mg/kg에서 40%의 부종이 억제되었다.

이 후, 전호잎 열수추출물의 항염증 효과를 기반으로 하여 랫트 초대배양 연골세포에서 염증에 대한 연골보호효과를 평가한 결과, 전호잎 열수추출물의 전처리는 염증에 의해 증가된 nitrite와 PGE_2의 생성을 감소시켰으며, iNOS, COX-2, MMP-3과 MMP-13의 mRNA 발현과 단백 발현 수준을 농도-의존적으로 감소시켰다. 그리고 전호잎 열수추출물은 염증에 의해 증가된 또 다른 연골기질분해 효소인 ADAMTS-4의 단백 발현을 유의적으로 감소시켰다. 게다가, 전호잎 열수추출물의 전처리는 염증에 의한 aggrecan,

collagen type II와 당아미노글리칸의 분해를 억제하였다. 염증이 유도된 랫트 초대배양 연골세포에서 전호잎 열수추출물의 연골보호 효과는 MAPKs(ERK, JNK, p38 MAPKs)의 인산화 억제와 IκB-α의 인산화 및 분해 억제를 통한 NF-κB의 subunit인 p65의 핵으로의 이동 억제에 의해 매개될 수 있음을 확인하였다. 생체 내 연구에서 전호잎 열수추출물의 연골보호효과를 검증하기 위해 DMM 수술을 받은 퇴행성관절염 실험동물에 전호잎 열수추출물을 8주 동안 매일 경구투여 한 후 조직학적 검사를 한 결과, 음용수를 받은 퇴행성관절염 실험군의 연골과 비교하여 8주 동안 전호잎 열수추출물을 받은 퇴행성관절염 실험군의 연골에서 연골 파괴가 억제되었으며 프로테오글리칸이 보호되어 있음을 확인하였다.

HPLC 분석을 통해 전호잎 열수추출물에서 chlorogenic acid, cynaroside와 luteolin-7-O- malonylglucoside를 동정하였으며 이 중 cynaroside가 전호잎 열수추출물의 염증에 대한 연골보호효과에 기여하고 있음을 iNOS, COX-2, TNF-α, MMP-13, ADAMTS-4, 그리고 aggrecan의 단백발현을 통해 확인하였다. 또, 프로테오글리칸에 대한 cynaroside의 보호효과는 알시안 블루 염색을 통해 확인하였으며, 그 결과 IL-1β처리 군과 비교하였을 때 cynaroside의 전처리는 염증에 의한 프로테오글리칸의 분해를 억제하였다.

이러한 결과들은 전호잎 열수추출물이 탁월한 항염증 및 연골보호효과를 가지고 있으며 이는 퇴행성관절염의 진행을 완화시키기 위한 예방 및 치료제로써 강력한 잠재력이 있음을 보여준다. 또, 이러한 전호잎 열수추출물의 효과는 향후 퇴행성관절염 예방 및 치료제로써의 개발 가능성을 시사한다.

I. Introduction

OA is a common degenerative joint disease following joint trauma and aging in elderly population, characterized by articular cartilage destruction, subchondral bone remodeling, pain, and osteophyte formation [1,2]. At the molecular level, the multifactorial pathogenesis of OA is related to oxidative and nitrosative stress by overproduction of ROS and RNS, inflammation by increased expression of inflammatory mediators, and cartilage matrix degradation by cartilage-degrading enzymes and inflammation [3]. In particular, cartilage matrix degradation by inflammation is known as the main cause [3]. Inflammation represents critically important responses of the host defense mechanism, which protects against endogenous and/or exogenous stimuli, however, excessive or persistent inflammation leads to chronic disease, including inflammatory arthritis, asthma, and multiple sclerosis [4]. IL-1β, a pro-inflammatory cytokine, is one of the potent inducers that accelerates the development of OA through releasing of cartilage degrading enzymes and inflammatory mediators, such as MMPs, ADAMTS, NO, and PGE_2 [5]. Elevated levels of IL-1β have been found in the synovial fluid and cartilage tissue of OA patients [6]. Among these matrix-degrading enzymes, the MMPs family plays a central role in cartilage degradation in OA [7]. In particular, MMP-13 is key player in the catabolic processes of OA. It not only hydrolyzes COL2A1 and aggrecan, which are essential constituents of the ECM of articular cartilage, but also degrades proteoglycan, collagent type Ⅳ and type Ⅸ, osteonectin and perlecan of cartilage ECM [8-10]. Clinical investigation revealed that patients with articular cartilage destruction have high MMP-13 expression, and other studies shown that *MMP-13*-overexpressing transgenic mice develop a spontaneous OA-like articular cartilage destruction phenotype [10-12]. In addition, ADAMTS-4 and -5, further key enzymes of ECM degradation, decompose aggrecan [13]. The degradation products of COL2A1 and aggrecan induce activation of synoviocytes and release

catabolic factors, resulting in promoting the paracrine secretion of pro-inflammatory cytokines and MMPs into the synovial fluid [14,15]. These repetitive vicious cycles of inflammation and catabolism cause cartilage degradation, proteoglycan loss, and neuropathic pain, resulting in uncomfortable motility.

Currently, for symptomatic relief of OA, including controlling pain and improving the movement, NSAIDs and analgesics as pharmacological drugs, or joint replacement surgery are commonly used [16,17]. However, long-term use of these drugs leads to side effects such as gastrointestinal toxicity and weakened kidney function, rather than slowing down or reversing the progression of OA [16]. Nutraceuticals, such as glucosamine and chondroitin sulfate, have also been used to relieve OA symptoms [18,19]. However, recent studies on the latter have reported that it is not effective, either alone or combination with glucosamine, for therapeutic effects in humans [19,20]. Therefore, it is necessary to find new drugs that can delay OA progression or alleviate symptoms, and there have been recent efforts to identify candidates in traditional medicinal plants [3,7,21,22]. The reason is that they can produce bioactive components including various acidic and phenolic compounds, have minimal side effects, are easily consumable, and cheaper [3,11]. Musumeci *et al.* identified the beneficial effect of extra-virgin olive oil through the increase expression of luburicin, which is a chondroprotective glycoprotein, on ACLT surgery-induced degenerative articular cartilage in rats [23]. In addition, they reported that oleic acid, which accounts for 78% of extra-virgin olive oil, inhibits ROS produced by exhaustive exercise, leading to rapid recovery of damaged muscle tissues in rats [24]. As described above, studying various mechanisms with natural substances and demonstrating the anti-arthritic effect, which can increase the possibility of development of anti-osteoarthritic, its usefulness is very high.

Anthriscus sylvestris (L.) Hoffm. (Apiaceae) is a wild perennial plant which grows in hedges, road verges, and neglected pastures in Europe, Asia, and New

Zealand [25,26]. *A. sylvestris* has been used in traditional medicine, for example as an antipyretic and to treat coughs and diuretic in Asia [27], to treat headaches in Ireland and Tunisia [28,29], and to treat rheumatism and other inflammatory ailments in India [30]. Several studies analyzed the major components in extracts of the aerial parts of *A. sylvestris*; major antioxidant components of ethanol extracts were quercetin and apigenin, and the methanol extracts were luteolin-7-O-glucoside (cynaroside) and chlorogenic acid [31,32]. However, studies on the physiological active function of the AE-ASL, which has various components, have not been reported except for the anti-proliferative, and antioxidant properties. Therefore, the purpose of this study was to evaluate the chondroprotective effect and underlying mechanisms *in vitro* and *in vivo* to verify the utility of AE-ASL as an anti-arthritis agent.

II. Materials and Methods

1. Materials

1.1. Preparation of AE-ASL

Dried *A. sylvestris* leaves (1 kg), purchased from Heuksando, Republic of Korea, were ground and extracted in 45.5 volumes of water (v/w) at 90°C for 3 h, followed by filtration utilizing a 55 μm bag filter. The extract was concentrated in a centrifugal-flow-thin-film vacuum evaporator (Okawara, Shizuoka, Japan) and lyophilized (CUDDON, New Zealand). The dried extract (293 g) was dissolved in distilled water (100 mg/mL), and the solution was filtered through a 0.45 μm filter. The extract was stored at −20°C until use. The yield of the aqueous extract was about 29.3% (w/w).

1.2. Reagent

1.2.1. Cell culture

DMEM, DMEM/F12 and 100 U/mL penicillin and 100 mg/mL streptomycin solution were purchased from WelGene (Daegu, Republic of Korea). FBS was purchased from Corning (Corning, NY, USA). Collagenase type II was purchased from Worthington Biochemical Corp. (Lakewood, NJ, USA).

1.2.2. Efficacy evaluation in cells

IL-1β was purchased from ProSpec-Protein Specialists (Rehovot, Israel). Sulfanilamide, MTT, LPS, N-(1-naphthyl) ethylenediamine dihydrochloride,

phosphoric acid, casein, cynaroside, DMMB, and chondroitin were purchased from Sigma-Aldrich Corp. (St.Louis, MO, USA). The aggrecan ELISA kit and COL2A1 ELISA kit were purchased from MyBioSource (SanDiego, CA, USA) and the PGE_2 ELISA kit was purchased from R&D Systems (Minneapolis, MN, USA). Primary and secondary antibodies were purchased from Cell Signaling Technology (Danvers, MA, USA), except for the anti-inducible nitric oxide synthase (Abcam, Cambridge, MA, USA) and anti-β-actin (AB Frontier, Seoul, Republic of Korea).

1.2.3. Component analysis of AE-ASL

Methanol, acetonitrile and water of HPLC grade obtained from Fisher Scientific (Fair Lawn, JN, USA). All other common chemicals and solvents were analytical reagent grade or HPLC-grade.

1.2.4. Efficacy evaluation in experiment animals

Carrageenan, diclofenac sodium, safranin O, fast green FCF were purchased from Sigma-Aldrich Corp. (St.Louis, MO, USA). Ethanol and xylene were purchased from Duksan pure chemical (Gyeonggi-do, Republic of Korea).

2. Methods

2.1. Cell culture

2.1.1. Murine macrophage RAW264.7 and induction of inflammation

Murine macrophage RAW264.7 cells were obtained from the Korea Research

Institute of Bioscience and Biotechnology (Daejeon, Republic of Korea). Cells were cultured in DMEM containing 10% FBS and antibiotics in a humidified incubator with 5% CO_2 at 37°C. LPS (0.2 μg/mL) was used to induce inflammation in RAW264.7 cells.

2.1.2. Rat chondrocytes isolation and induction of inflammation

Five-day-old postnatal Sprague-Dawley rats were sacrificed. Under sterile conditions, dissected knee cartilage of rats was enzymatically digested with 0.3% (w/v) collagenase type II dissolved in DMEM/F12, for 45 min at 37°C with gently stirring, repeated twice. Thereafter, once again, the cartilage was digested with 0.3% (w/v) collagenase type II for 5 h at 37°C with gently stirring. Cells and debris that could not be digested even after the enzymatic digestion reaction were filtered by cell strainer (0.45 μm), and then chondrocytes were separated. Chondrocytes were cultured in DMEM/F12 containing 10% FBS and antibiotics in a humidified incubator with 5% CO_2 at 37°C. Separated chondrocytes were seeded in 6-well or 12-well cell culture plates according to the purpose of the experiment, and further cultured for 3 days for cell stabilization. On the day before the experiment, the medium was replaced with DMEM/F12 containing 1% FBS, and cultured for 12 h. and then sample was treated. IL-1β (20 ng/mL) was used to induce inflammation in chondrocytes.

2.2. Cell viability assay

RAW264.7 cells and isolated chondrocytes were seeded at 1×10^6 cells/mL in 12-well culture plates, incubated for 12 h and 24 h, respectively, and then treated with varying concentration of AE-ASL for 24 h. Following incubation, MTT (0.5 mg/mL) reaction was performed for 4 h, generated formazan was dissolved in DMSO, and then measured absorbance at 590 nm in a microplate

reader (Epoch; BioTek Instruments, Winooski, VT, USA). The results was expressed as the cell viability rate by setting the absorbance of untreated control cells to 100%. The treated cell viability was calculated using the following formula:

$$Cell\,viability\,(\%) = \frac{Means\,Abs.\,of\,the\,sample - Means\,Abs.\,of\,the\,blank}{Means\,Abs.\,of\,the\,control - Means\,Abs.\,of\,the\,blank} X100$$

2.3. Measurement of nitrite and PGE_2 production

RAW264.7 cells and isolated chondrocytes were seed at 1×10^6 cells/mL in a 12-well culture plate. The cells were pretreated with varying concentrations of AE-ASL (RAW264.7 cells; 10, 25, 50, and 100 μg/mL, Chondrocytes; 0.5, 1, and 2 mg/mL) for 1 h, and then subsequently cultured with LPS (0.2 μg/mL) and IL-1β (20 ng/mL), respectively, for 24h. NO production was determined by measuring the accumulation of nitrite (NO_2^-), the stable oxidation product of NO, using Griess reagent. In brief, 100 μl of cell culture medium was mixed with 100 μl of Griess reagent [1% sulfanilamide and 0.1% naphthylethylenediamine dihydrochloride in 2.5% phosphoric acid], and incubated at room temperature for 5 min. The absorbance was measured at 540 nm using a microplate reader (Epoch Bioteck, Bio-Tek Instruments Inc., Winooski, VT, USA). Fresh culture medium was used as a blank in every experiment. The quantity of nitrite was determined in comparison with a sodium nitrite standard curve. The production of PGE_2 in the culture medium was quantified using a Parameter™ prostaglandin E_2 assay kit, according to manufacturer's protocol.

2.4. Isolation of total RNA and RT-PCR

Isolation of total RNA was performed using Trizol reagent (GeneAll, Seoul,

Republic of Korea). RNA (1 μg) was reverse-transcribed using Moloney Murine Leukemia Virus reverse-transcriptase (Enzynomics, Daejeon, Republic of Korea) and then amplified by PCR (Applied biosystems®) using specific primers shown in Table 1. The PCR products were subject to agarose gel electrophoresis to measure the induction of expression of specific genes. *Glyceraldehyde 3-phosphate dehydrogenase (GAPDH)* was used as an internal control for normalization.

Table 1. Specific primer sequences.

Species	Gene name	Sequence (5'→3')		Size (bp)
Mouse	*iNOS*	F	GACCTTTCGCATTAGCATGGAAGC	709
		R	TTGTGCATCGACCTAGGCTGGAA	
	COX-2	F	GTGAATGCCACCTTCATCCGAGAA	320
		R	CACGCGGTTATGTTCACGAAGCCA	
	TNF-α	F	TGGAACTGGCAGAAGAGGCA	518
		R	TGCTCCTCCACTTGGTGGTT	
	IL-1β	F	GGCAGGCAGTATCACTCATT	352
		R	CCCAAGGCCACAGGTATTT	
	IL-6	F	TGCAAGAGACTTCCATCCAGTTGC	358
		R	CCAGGTAGCTATGGTACTCCAG	
	GAPDH	F	ACTCACGGCAAATTCAACGGCAC	382
		R	GGACTGTGGTCATGAGCCCTTCCA	
Rat	*iNOS*	F	TTCCTCACTGGGACTGCACA	323
		R	AGCCTGGCCAGATGTTCCTC	
	COX-2	F	ACCATCTGGCTTCGGGAGCACAA	576
		R	GAGGGCTTTCAACTCTGCAGCCA	
	MMP-3	F	TCCTACCCATTGCATGGCAGTGAA	497
		R	GCATGAGCCAAGACCATTCCAGG	
	MMP-13	F	GGCAAAAGCCATTTCATGCTCCCA	562
		R	AGACAGCATCTACTTTGTCGCCA	
	GAPDH	F	TGGTGCTGAGTATGTCGTGGAGTC	578
		R	AGACAACCTGGTCCTCAGTGTAGC	

2.5. Protein isolation and western blot analysis

RAW264.7 cells and isolated chondrocytes were pretreated with AE-ASL for 1 h and stimulated with LPS (0.2 μg/mL) and IL-1β (20 ng/mL), respectively, for 24 h. To extract whole intracellular proteins, cells lysed with a PRO-PREP protein extraction solution (iNtRON Biotechnology, Republic of Korea) were incubated for 30 min on ice. The supernatants were transferred to new tubes after centrifugation at 15,000 *g* for 15 min at 4°C. Cytoplasmic and nuclear proteins were extracted using NE-PER™ nuclear and cytoplasmic extraction reagents (Thermo Scientific, IL, USA), according to the manufacturer's instructions. Protein concentrations in each lysate were quantified using a BCA protein assay kit (Pierce, Rockford, IL, USA). Proteins (20 μg) were separated by 10%, 12% or 15% SDS-PAGE and then transferred onto PVDF membranes (Bio-Rad Laboratories, Hercules, CA, USA). The transblotted membranes were blocked with 5% bovine serum albumin in TBST for 1 h. Subsequently, the membranes were incubated with specific primary antibodies at 4°C overnight followed by incubation for 1 h with a HRP-conjugated secondary antibody at room temperature. The immunoreactive bands were developed using an ECL kit (Millipore, Bedford, MA, USA) and visualized using a MicroChemi 4.2 imager (DNR Bioimaging Systems, Jerusalem, Israel).

2.6 Casein zymography

Cultured media (30 μL) was mixed with non-reducing sample buffer (250 mM Tris-HCl (pH 6.8), 40% (v/v) glycerol, 8% (w/v) SDS, 0.01% (w/v) bromophenol blue) and resolved using 8% SDS-PAGE containing co-polymerized casein. After electrophoresis, gels were placed in PBS containing 2.5% (v/v) Triton X-100 for 30 min gently shaking, and washed with cold PBS for 15 min three times. The gels were incubated with zymogram renaturing buffer (10 mM $CaCl_2$, 50 mM

Tris-HCl (pH 7.6), 0.15 M NaCl) at 37°C for 72 h. After renaturation of the cartilage-degrading enzymes, gels were stained with 0.1% (w/v) Coomassie brilliant blue R-250, followed by destaining until clear bands were visible, at which time they were photographed with a digital camera (G16, Canon, Tokyo, Japan).

2.7 DMMB assay

To quantify sGAG content, chondrocytes were pretreated with AE-ASL for 1 h, and then subsequently cultured with IL-1β (20 ng/mL) for 24 h. The cultured media was mixed with DMMB solution (40 mM NaCl, 40 mM Glycine, 46 μM DMMB) at 1:10, and absorbance measured at 525 nm within 10 min using a microplate reader. Bovine cartilage chondroitin sulfate was used as a standard curve for sGAG contents.

2.8. Aggrecan and COL2A1 ELISA analysis

Rat primary chondrocytes were seeded at 1×10^6 cells/mL in 6-well culture plates. Chondrocytes were pretreated with AE-ASL for 1 h, and then subsequently cultured with IL-1β (20 ng/mL) for 24 h. After incubation for 24 h, the supernatant of each sample was collected to assess aggrecan and COL2A1 content, using aggrecan ELISA and COL2A1 ELISA kits respectively, according to manufacturer's protocol.

2.9 Alcian blue staining

Rat primary chondrocytes were seeded at 1×10^6 cells/mL in 6-well culture plates. Chondrocytes were pretreated with cynaroside for 1 h, and then subsequently cultured with IL-1β (20 ng/mL) for 48 h. After washing with PBS,

cells fixed with 70% EtOH, and stained with 0.1% Alcian blue 8GX in 0.1 N Hcl for 6 h at room temperature. After washing with PBS, each well was photographed with a digital camera (G16, Canon, Tokyo, Japan).

2.10 HPLC analysis

The extract sample was analyzed using a Shimadzu HPLC system equipped with a photo diode array (PDA) (Shimadzu, Kyoto, Japan). The sample solutions (1 mg/mL) were separated using a 5C18 MS ll column (4.6 mm i.d. × 250 mm; Cosmosil, Japan) at 40°C. The mobile phase was a mixture of two liquids distributed by the 0.1% TFA/DW (A) and 0.1% TFA/MeCN (B) at a flow rate 1.0 mL/min. The gradient elution program was used as follows: 90% A (0.5 min), 15% A (30 min), 5% A (40 min), 90% A (40.1 min). The injection volume was 10 μL, and detection was at wavelength of 320 nm. The mass measurement of compounds (1, 2, and 3) was analyzed using Nexera X2 HPLC system coupled to LCMS-IT-TOF (Shimadzu, Kyoto) included a CBM-20A system controller, LC-30AD pump, a SIL-20AC autosampler, a CTO-30A column oven and a SPD-M30A diode array detector with a Capcell Core C18 Column (Shiseido, Kyoto, Japan). The gradient program was used with the mobile phase, combining 0.1% TFA/DW (A) and 0.1% TFA/MeCN (B) as follows: 90% A (0.5 min), 15% A (20 min), 5% A (25 min), 90% A (25.1 min). The parameters were as follows: flow rate, 0.2 mL/min; injection volume, 5 uL; wavelength, at 320 nm; voltage, 4.50 kV as ESI positive mode; CDL temperature, 200°C; block heater temperature, 200°C; nebulizer gas flow, 1.5 L/min; ion accumulation time, 10 msec. All data were recorded and analyzed by Shimadzu software; LCMS solution ver. 3.60, Formula Predictor Ver. 1.2, and Accurate Mass Calculator (Shimadzu, Kyoto, Japan).

2.11 *In vivo* study

2.11.1. Animals

Male Sprague-Dawley rats (8 weeks old) were purchased from Damool Science (Daejeon, Republic of Korea). They were housed in plastic cages in temperature (21 ± 1°C)- and humidity (55 ± 5%)-controlled room with a 12-h light/dark cycle. Animals were allowed access to water and pellet chow *ad libitum*. All animal handling procedures were in accordance with the National Institutes of Health Guide for the Care and Use of Laboratory Animals [33].

2.11.2. Generation of carrageenan-induced paw edema in rats

All animal care and procedures were controlled and approved by the Chosun University Institutional Animal Care and Use Committee (CIACUC2017-A0011). The rats were acclimated for 1 week for environment adaptation before the experiment. The rats were randomly divided into six groups (n = 4 each): group 1 (normal, 0.9% normal saline), group 2 (paw edema, 0.9% normal saline), groups 3–5 (paw edema, 50, 100, and 200 mg/kg AE-ASL, respectively), and group 6 (paw edema, 10 mg/kg diclofenac sodium). The edema was induced by subcutaneous injection of 0.1 mL of a 1% (w/v) carrageenan type IV suspension in 0.9% normal saline into the left hind paw 1 h after oral administration of AE-ASL. The paw thickness was measured in the middle of the paw using a digital caliper before (time 0) and at different time points (up to 24 h) after carrageenan injection, as described previously [34]. The percentage anti-inflammatory activity (AA%) was calculated using the following formula [34]:

$$AA\,(\%) = \frac{(C_t - C_0)control - (C_t - C_0)treated}{(C_t - C_0)control} X100$$

Where,

C_t = left hind paw thickness (mm) at time t.

C_0 = left hind paw thickness (mm) before carrageenan injection.

(C_t-C_0)control = increase in rat paw size after carrageenan injection at time t.

(C_t-C_0)treated = increase in paw size after carrageenan injection in reference or test drug-treated rats at time t.

2.11.3. Generation of DMM-induced OA models in rats

All animal care and procedures were controlled and approved by the Chosun University Institutional Animal Care and Use Committee (CIACUC2016-S0029). The rats were acclimated for 1 week for environment adaptation before the experiment. The rats (*n* = 24) were randomly divided into the following six groups of four rats each and treated as indicated: Group 1 (Normal), Group 2 (Sham, 0.9% normal saline), Groups 3 (DMM, 0.9% normal saline), Group 4-6 (DMM, 50, 100, and 200 mg/kg body weight, AE-ASL, respectively). For DMM surgery, rats were anesthetized with 2.5% isoflurane, and underwent surgical operation to MMTL on the right and left knees to induced OA [35]. For sham surgery, MMTL was visualized but not transected. The day after the DMM surgery, AE-ASL groups were orally administered with AE-ASL (50, 100, and 200 mg/kg) daily for 8 weeks and the OA and sham group were orally administered saline. All rats were sacrificed the day after the final administration.

2.11.4. Histology analysis and score

Knee joint samples were fixed in 10% neutral buffered formalin, decalcified with 0.5 M EDTA (pH 7.4), dehydrated through a series of ethanol solutions, and embedded in paraffin blocks. After that, lateral serial sections were cut 4 μm intervals, and stained with Harris Hematoxylin-Eosin and Safranin-O/Fast Green.

The stained sections were scored based on the Osteoarthritis Research Society International (OARSI) advanced Osteoarthritis Cartilage Histopathology Assessment System (0-6.5), and used a summed OARSI score to evaluate the degree of articular cartilage destruction [36].

2.12. Statistical analysis

All data were derived from at least three independent experiments (except the *in vivo* study). The results are expressed as the means ± standard deviation (SD). A one-way analysis of variance, followed by Dunnett's test, was used for multiple comparisons using GraphPad Prism (GraphPad Software, CA, USA). The p-value < 0.05 were considered statistically significant in each test.

Ⅲ. Results

3. Evaluation of anti-inflammatory efficacy in mouse macrophage RAW264.7 cells and carrageenan-induced paw edema rat models

3.1 Effect of AE-ASL on viability of RAW264.7 cells

The MTT assay was used to evaluate the cytotoxicity of AE-ASL in RAW264.7 cells. As shown in Figure 1, AE-ASL did not exhibit cytotoxic effects up to 100 μg/mL. However, at a higher concentration (200 μg/mL), AE-ASL decreased the cell viability by approximately 30%. Therefore, all further experiments were performed at concentrations of up to 100 μg/mL to avoid cytotoxicity.

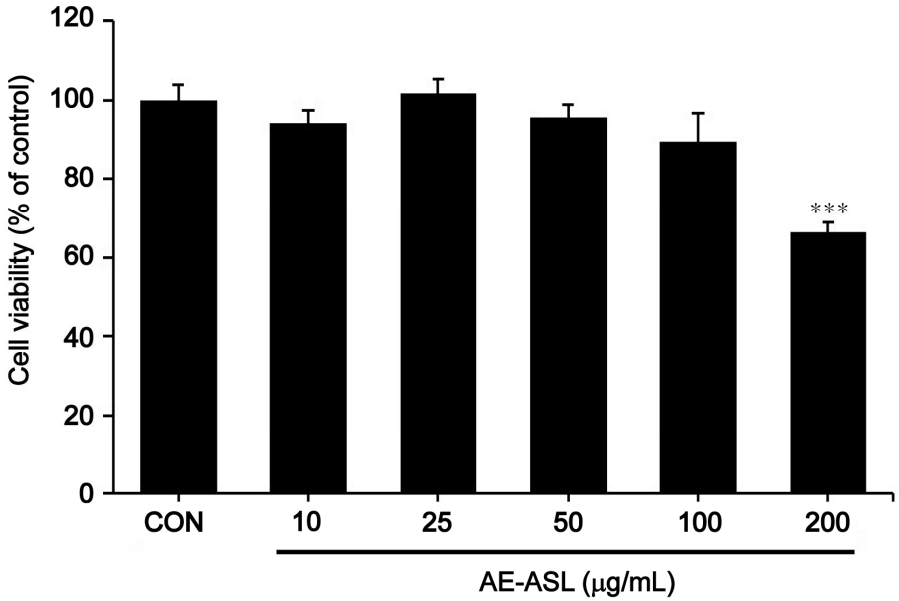

Figure 1. Effects of AE-ASL on cell viability of RAW264.7 cells. Cells were treated with various concentrations of AE-ASL (10, 25, 50, 100, and 200 μg/mL) for 24 h. Cell viability was determined using an MTT assay, and the results were expressed as the percentage of control. Data are the means ± SD of three independent experiments. ***$p < 0.001$ compared to the control group.

3.2 AE-ASL inhibited nitrite production and iNOS expression in LPS-stimulated RAW264.7 cells

LPS alone significantly increased the nitrite production by 18-fold (18.14 ± 0.52 μM) compared with that in the control (0.599 ± 1.01 μM, Figure 2A). However, pretreatment with AE-ASL inhibited the LPS-induced nitrite production in a dose-dependent manner, by 30% (14.48 ± 0.52 μM), 60% (6.15 ± 1.0 μM), and 80% (3.24 ± 0.52 μM) at 25, 50, and 100 μg/mL, respectively (Figure 2A). To elucidate the inhibitory effects of AE-ASL on the LPS-induced nitrite production, mRNA and protein expression levels of iNOS were evaluated using RT–PCR and western blotting. As shown in Figure 2B-D, LPS alone significantly increased both mRNA and protein expression levels of iNOS. However, pretreatment with AE-ASL for 1 h inhibited the LPS-induced mRNA and protein expression of iNOS in a dose-dependent manner, by 80% and 86% at 100 μg/mL, respectively (Figure 2B-D). Taken together, these data suggest that the AE-ASL-mediated inhibition of nitrite production was associated with the regulation of iNOS expression in the LPS-stimulated RAW264.7 cells.

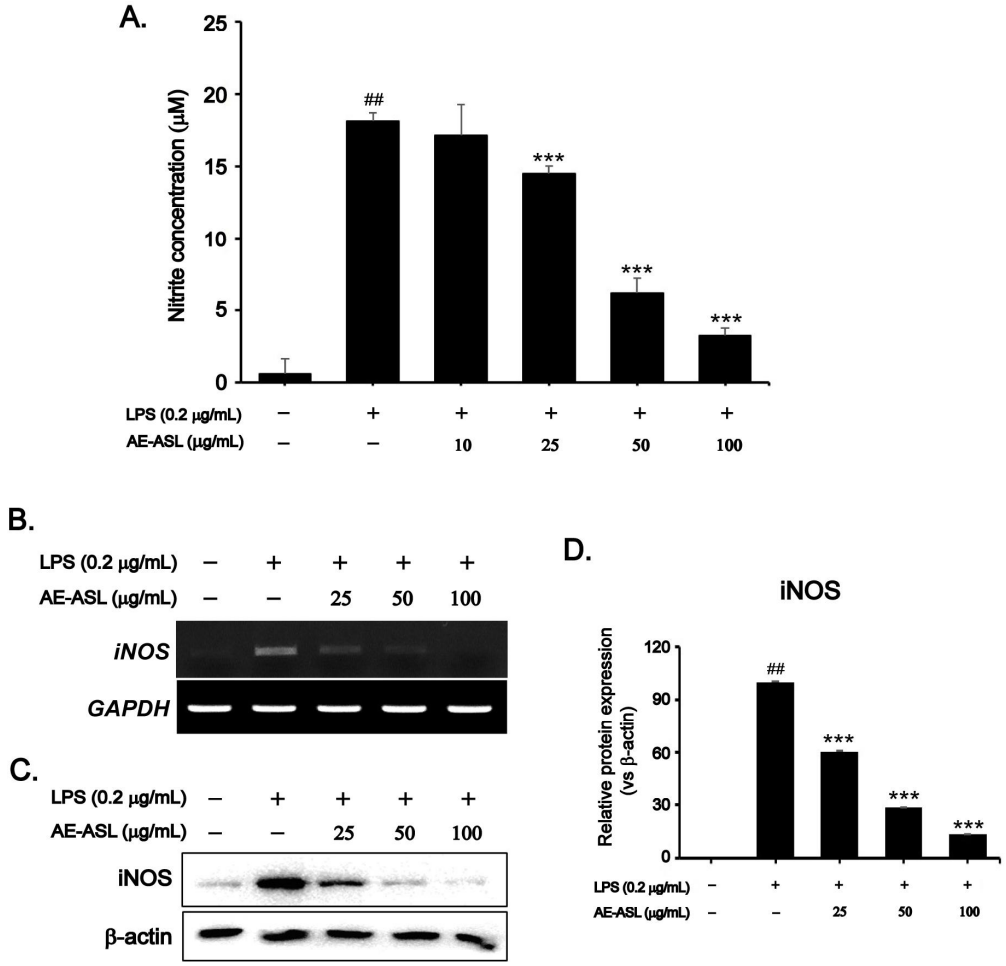

Figure 2. Inhibitory effects of AE-ASL on LPS-induced nitrite production and iNOS expression in RAW264.7 cells. Cells were pretreated with AE-ASL (10, 25, 50, and 100 μg/mL) for 1 h, followed by LPS (0.2 μg/mL) stimulation for 24 h**.** (A) Nitrite production was determined in the cell culture supernatant using the Griess reagent after 24 h. (B and C) Expression levels of the iNOS mRNA and protein was determined using RT–PCR and western blot analysis. (D) Quantitative data of (C) were analyzed using the ImageJ software. *GAPDH* and β-actin served as internal controls, respectively. Results are the means ± SD of three independent experiments. ##$p < 0.01$ compared to the control group; ***$p < 0.001$ compared to the LPS-treated group.

3.3 AE-ASL inhibited PGE_2 production and COX-2 expression in LPS-stimulated RAW264.7 cells

PGE_2 (produced by COX-2) is one of the key pro-inflammatory mediators of inflammation-related diseases [5]. The quantitative analysis of PGE_2 using ELISA showed that LPS treatment of RAW264.7 cells promoted the generation and release of PGE_2 into the supernatant by 2-fold (1,700.42 ± 9.39 pg/mL) compared with that in the control (808.48 ± 90.72 pg/mL, Figure 3A). However, pretreated with AE-ASL for 1 h inhibited the LPS-induced PGE_2 production in a dose-dependent manner, by 10% (1,600.12 ± 12.3 pg/mL), 15% (1,483.07 ± 40.6 pg/mL), and 35% (1,100.40 ± 45.57 pg/mL) at 25, 50, and 100 μg/mL, respectively (Figure 3A). To elucidate the inhibitory effects of AE-ASL on the LPS-induced PGE_2 production, mRNA and protein expression levels of COX-2 were evaluated using RT–PCR and western blotting. As shown in Figure 3B-D, LPS alone significantly increased both the mRNA and protein expression levels of COX-2. However, pretreatment with AE-ASL for 1 h inhibited the LPS-induced mRNA and protein expressions of COX-2 in a dose-dependent manner. Taken together, these data suggest that the AE-ASL inhibited the mRNA and protein expression of COX-2, which generates PGE_2 that functions as a key mediator of inflammation in LPS-stimulated RAW264.7 cells.

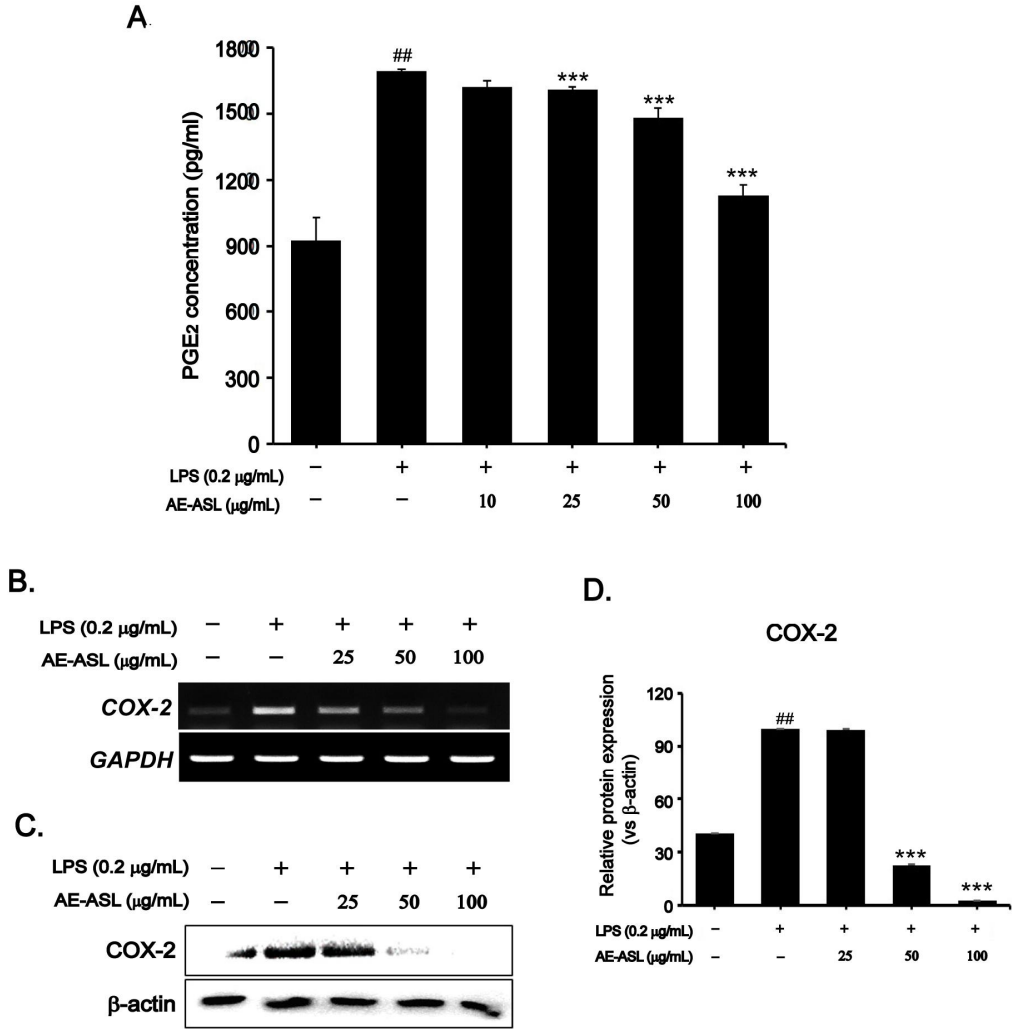

Figure 3. Inhibitory effects of AE-ASL on LPS-induced PGE_2 production and COX-2 expression in RAW264.7 cells. Cells were pretreated with AE-ASL (10, 25, 50, and 100 μg/mL) for 1 h, followed by LPS (0.2 μg/mL) stimulation for 24 h**.** (A) PGE_2 production was determined in the cell culture supernatant using an ELISA kit after 24 h. (B and C) Expression levels of the COX-2 mRNA and protein was determined using RT–PCR and western blot analysis. (D) Quantitative data of (C) were analyzed using the ImageJ software. *GAPDH* and β-actin served as internal controls, respectively. Results are the means ± SD of three independent experiments. ##$p < 0.01$ compared to the control group; ***$p < 0.001$ compared to the LPS-treated group.

3.4 AE-ASL inhibited expression of proinflammatory cytokines in LPS-stimulated RAW264.7 cells

Since AE-ASL inhibited nitrite and PGE_2 production, its effects on the expression of proinflammatory cytokines such as TNF-α, IL-1β, and IL-6, which play important roles in immune responses, were evaluated. As shown in Figure 4, LPS stimulation led to significant increases in them mRNA and protein levels of TNF-α, IL-1β, and IL-6 compared with those in the control. However, pretreatment with AE-ASL at 100 μg/mL inhibited the LPS-induced mRNA expressions of TNF-α, IL-1β, and IL-6 by 76%, 73%, and 59%, respectively (Figure 4A and B). The protein expression levels were also inhibited upon exposure to 25–100 μg/mL AE-ASL (Figure 4C and D). These results suggest that AE-ASL significantly suppressed the LPS-induced TNF-α, IL-1β, and IL-6 expression, which indicate that AE-ASL has anti-inflammatory activity.

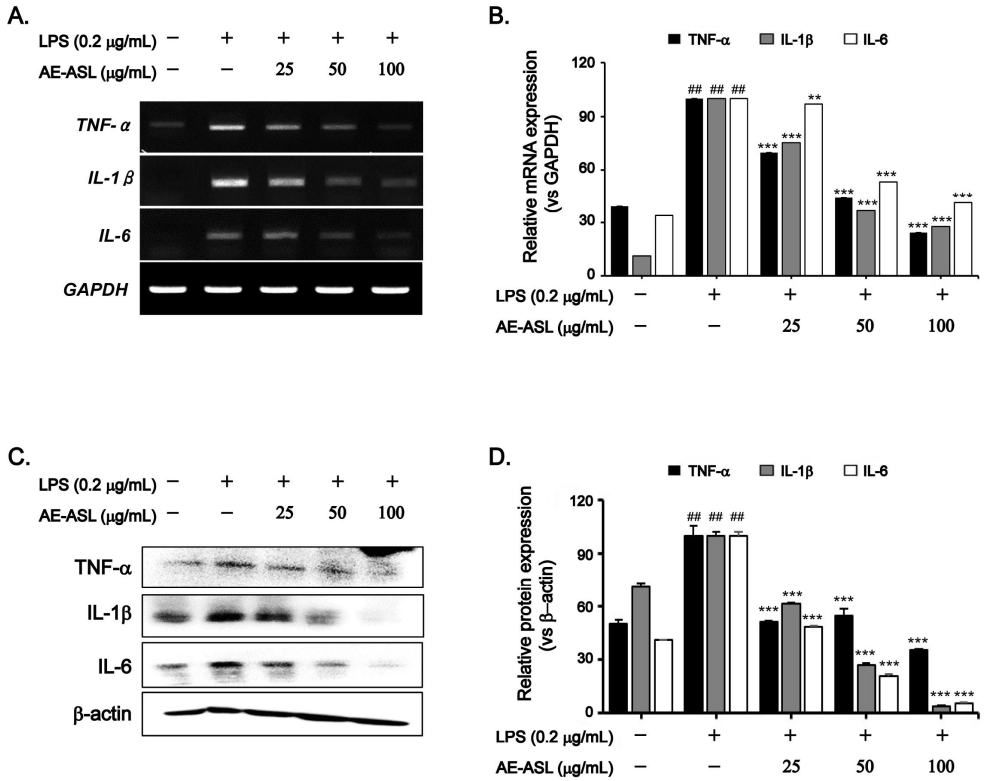

Figure 4. Inhibitory effects of AE-ASL on LPS-induced proinflammatory cytokines expression in RAW264.7 cells. Cells were pretreated with AE-ASL (25, 50, and 100 μg/mL) for 1 h, followed by LPS (0.2 μg/mL) stimulation for 24 h. (A and C) Expression levels of the TNF-α, IL-1β, and IL-6 mRNA and protein was determined using RT–PCR and western blot analysis. *GAPDH* and β-actin served as internal controls, respectively. (B and D) Quantitative data of (A and C), respectively, were analyzed using the ImageJ software. Results are the means ± SD of three independent experiments. $^{\#\#}p < 0.01$ compared to the control group; $^{**}p < 0.01$ and $^{***}p < 0.001$ compared to the LPS-treated group.

3.5 AE-ASL inhibited phosphorylation of IκBα and NF-κB p65 nuclear translocation in LPS-stimulated RAW264.7 cells

NF-κB is a crucial transcription factor that controls gene expression associated with inflammation such as iNOS, COX-2, and TNF-α [37]. To assess NF-κB activity, the nuclear translocation of the NF-κB p65 subunit and IκBα phosphorylation and degradation were evaluated using western blotting. As shown in Figure 5A and B, LPS stimulation significantly increased the phosphorylation and degradation of IκBα, the inhibitor of NF-κB. However, AE-ASL pretreatment markedly reversed the phosphorylation and degradation of I κBα in a dose-dependent manner. Consistent with IκBα degradation, the translocation of NF-κB p65 from the cytosol to the nucleus markedly increased upon LPS stimulation (Figure 5C–E). However, the LPS-induced nuclear translocation of NF-κB p65 was significantly inhibited by AE-ASL pretreatment (Figure 5C–E). These results suggest that AE-ASL effectively suppresses the NF-κB signaling pathway via inhibition of IκBα degradation, preventing the nuclear translocation of the NF-κB p65 subunit in LPS-stimulated macrophages.

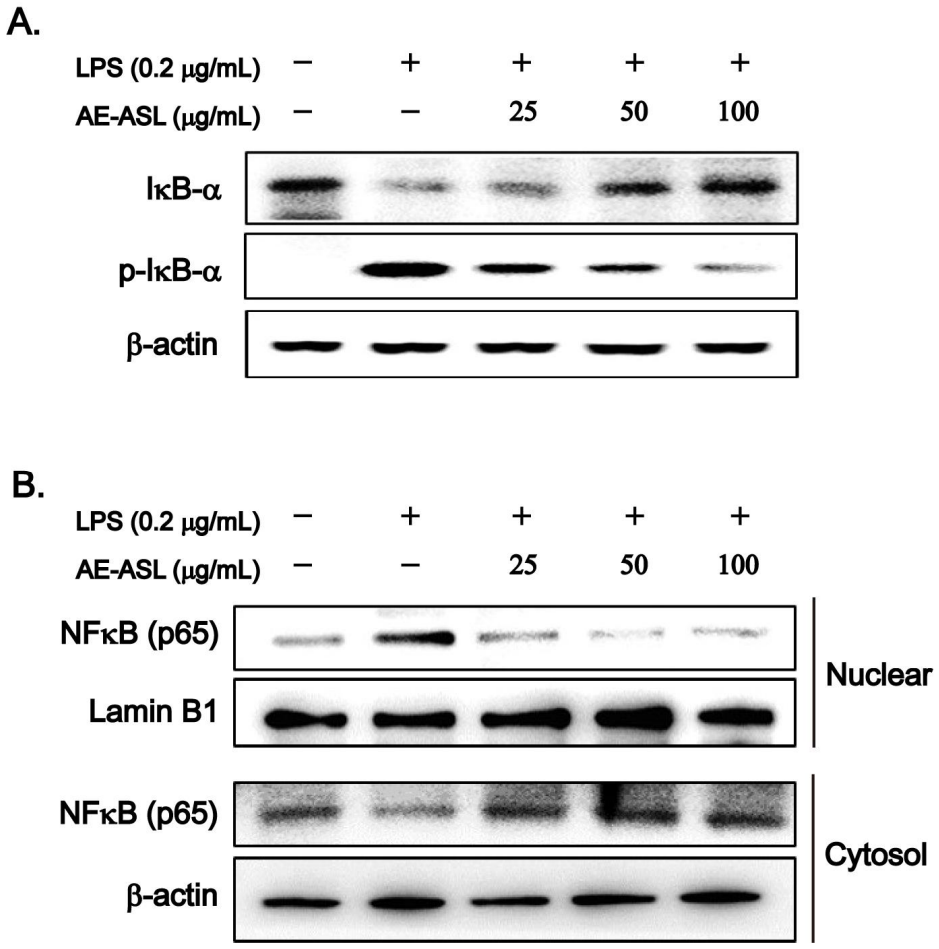

Figure 5. Effects of AE-ASL on LPS-induced phosphorylation of IκBα and NF-κB p65 nuclear translocation in RAW264.7 cells. Cells were pretreated with AE-ASL (25, 50, and 100 μg/mL) for 1 h, followed by LPS (0.2 μg/mL) stimulation for 1 h. (A) Protein levels of IκBα and phosphorylated IκBα were determined using western blotting. β-actin served as internal controls. (B) Protein levels of NF-κB p65 in nuclear and cytosolic extracts were determined using western blotting. β-actin and lamin B1 were used as cytosolic and nuclear internal controls, respectively.

3.6. AE-ASL inhibited phosphorylation of MAPKs in LPS-stimulated RAW264.7 cells

The activation of MAPK (ERK1/2, JNK, and p38 MPAK) modulates the activation of NF-κB in LPS-stimulated macrophages, affecting the transcriptional expression of iNOS [38]. To verify whether the inhibitory effect of AE-ASL on the LPS-induced activation of NF-κB and NO production is mediated through the MAPK pathway, the effect of AE-ASL on the LPS-induced phosphorylation of ERK, JNK, and p38 MAPK was evaluated by western blotting. Cells were pretreated with 0–100 μg/mL AE-ASL for 1 h and subsequently stimulated with LPS (0.2 μg/mL) for 1 h. Although phosphorylation of ERK1/2, JNK, and p38 MAPK significantly increased after exposure to LPS, pretreatment with AE-ASL at 100 μg/mL effectively decreased their phosphorylation, by 44%, 55%, and 26%, respectively (Figure 6). Meanwhile, the total expression levels of ERK1/2, JNK, and p38 MAPK were not significantly different among these groups. These results suggest that AE-ASL exerted its anti-inflammatory effects by inhibiting the activation of MAPKs during the LPS-induced inflammatory response.

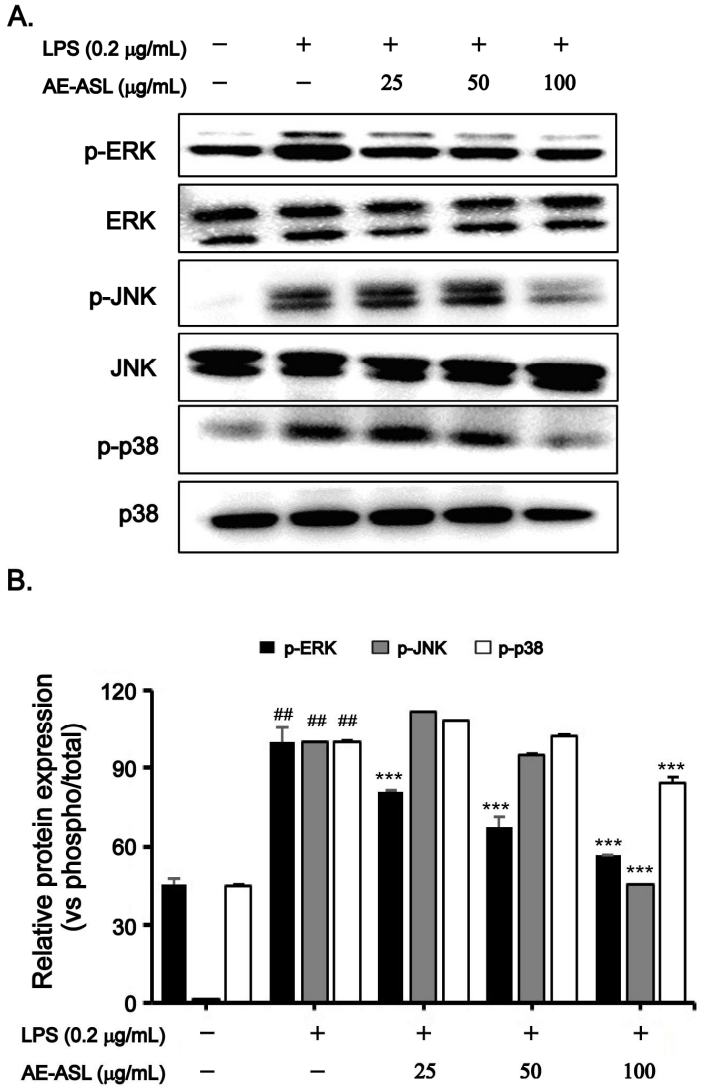

Figure 6. Effects of AE-ASL on LPS-induced phosphorylation of ERK, JNK, and p38 in RAW264.7 cells. Cells were pretreated with AE-ASL (25, 50, and 100 μ g/mL) for 1 h, followed by LPS (0.2 μg/mL) stimulation for 1 h. (A) Total and phosphorylated ERK, JNK, and p38 were determined using western blotting. (B) Quantitative data of (A) were analyzed using the ImageJ software. Results are the means ± SD of three independent experiments. ##p < 0.01 compared to the control group; ***p < 0.001 compared to the LPS-treated group.

3.7. AE-ASL inhibited carrageenan-induced rat paw edema

As shown in Figure 7B, AE-ASL (50, 100, or 200 mg/kg) and diclofenac sodium (positive control, 10 mg/kg), orally pre-administered 1 h before carrageenan injection, gradually increased the inhibition rate of the carrageenan-induced paw edema over a period of 24 h, compared with that in the untreated control group. At the high dose of AE-ASL (200 mg/kg), the inhibition of edema thickness was 27% and 40% at 2 h and 4 h after carrageenan injection, respectively, while diclofenac sodium showed 14% and 47% inhibition at 2 h and 4 h, respectively. Therefore, the anti-inflammatory effect of 200 mg/kg AE-ASL was comparable to that of diclofenac sodium (10 mg/kg). In addition, the middle dose (100 mg/kg AE-ASL) increased the inhibition of the edema thickness from 1% to 31% between 2 and 4 h after carrageenan injection (Figure 7B). The morphological characteristics are shown in Figure 7A.

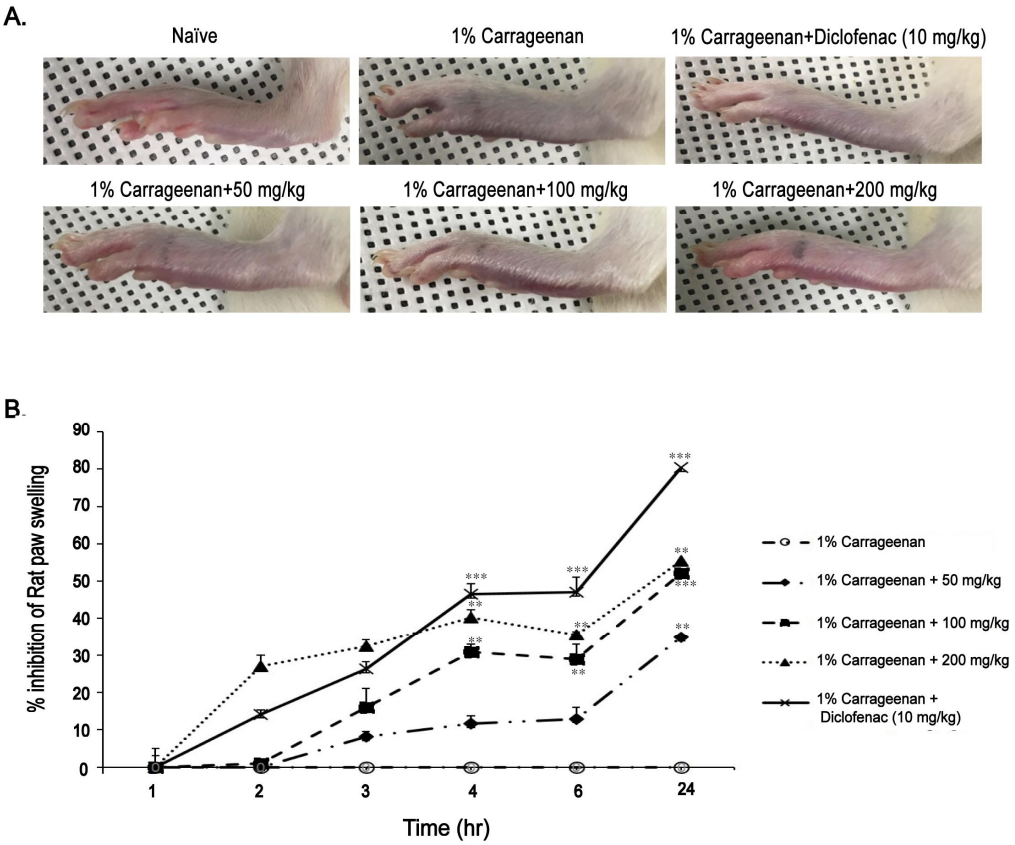

Figure 7. Effects of AE-ASL on carrageenan-induced left hind paw edema. Paw edema was induced by subcutaneous injection of a 1% carrageenan solution (100 μL/animal) into the left hind paw 1 h after oral administration of AE-ASL (50, 100, and 200 mg/kg) or diclofenac sodium (10 mg/kg). (A) Morphological characteristics of the left hind paw of rats 24 h after carrageenan injection. (B) The thickness of the paw was measured 0–24 h after carrageenan injection. Results are the means ± SD of four animals. $^{**}p < 0.01$ and $^{***}p < 0.001$ compared to the carrageenan group at the corresponding time points.

4. Evaluation of anti-osteoarthritic efficacy in rat primary chondrocytes and DMM-induced OA rat models

4.1. Effect of AE-ASL on the cell viability of rat primary chondrocytes

To evaluate the cytotoxicity of AE-ASL, chondrocytes were treated with various concentrations of AE-ASL (0.25, 0.5, 1, 2, and 4 mg/mL) and an MTT assay performed 24 h later. As shown in Figure 8, compared with the control, AE-ASL treatment of up to 2 mg/mL was not cytotoxic, but cell viability decreased by 80% at 4 mg/mL and the IC_{50} was 3.392 mg/mL. Therefore, the subsequent experiments were performed with 0.5, 1, and 2 mg/mL AE-ASL to avoid cytotoxicity.

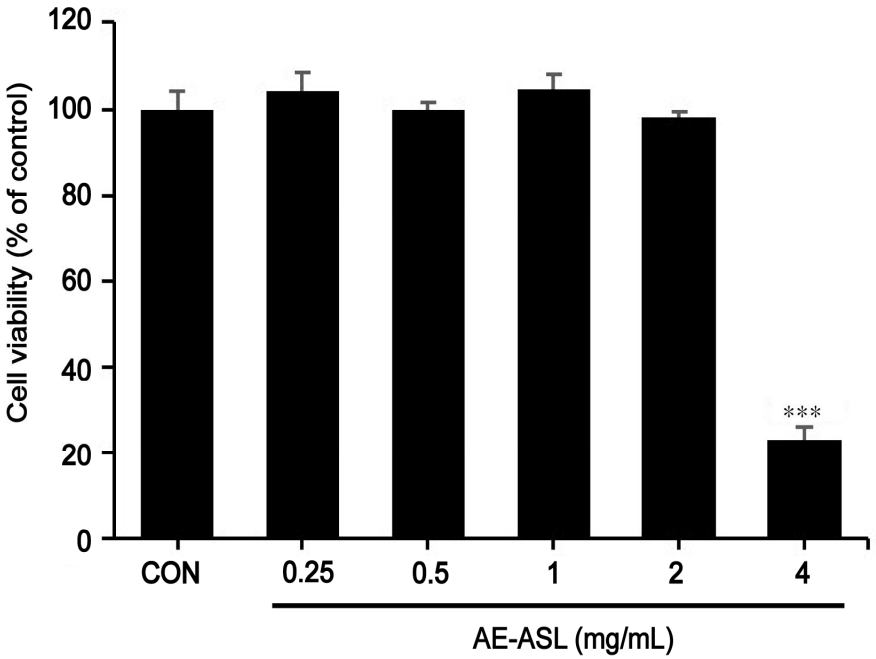

Figure 8. Effects of AE-ASL on the cell viability of rat primary chondrocytes. Cells were treated with various concentrations of AE-ASL (0.25, 0.5, 1, 2, and 4 mg/mL) for 24 h. Cell viability was determined using an MTT assay, and the results were expressed as a percentage of the control. Data are the means ± SD of three independent experiments. ***$p < 0.001$ compared with control group.

4.2. AE-ASL inhibited nitrite production and iNOS expression in IL-1β -stimulated rat primary chondrocytes

Inflammation by release of inflammatory mediators, such as nitrite oxide and iNOS is one of the major factors of osteoarthritis multi-factoretiology [3]. Therefore, the effect of AE-ASL on the IL-1β-induced both nitrite production and iNOS expression was evaluated in rat primary chondrocytes. Chondrocytes were pretreated with AE-ASL (0.5, 1, and 2 mg/mL) for 1 h and then stimulated with IL-1β (20 ng/mL) for 24 h. IL-1β alone significantly increased the nitrite production by 11-fold (55 ± 0.55 μM) compared with that in the control (5.43 ± 0.37 μM, Figure 9A). However, chondrocytes pretreated with AE-ASL inhibited IL-1β-induced nitrite production in a dose-dependent manner, by 35% (35.50 ± 0.37 μM), 67% (18.04 ± 0.18 μM), and 80% (10.88 ± 0.27 μM) at 0.5, 1, and 2 μg/mL, respectively (Figure 9B). In addition, IL-1β alone significantly increased both the mRNA and protein expression levels of iNOS. However, pretreatment with AE-ASL for 1 h inhibited the IL-1β-induced mRNA and protein expression of iNOS in a dose-dependent manner. (Figure 9B-D). In particular, at 2 mg/mL AE-ASL, the expression of iNOS proteins was completely suppressed, despite the presence of IL-1β (Figure 9C and D). These results suggest that AE-ASL-mediated inhibition of nitrite production was associated with the regulation of iNOS expression in IL-1β-stimulated rat primary chondrocytes.

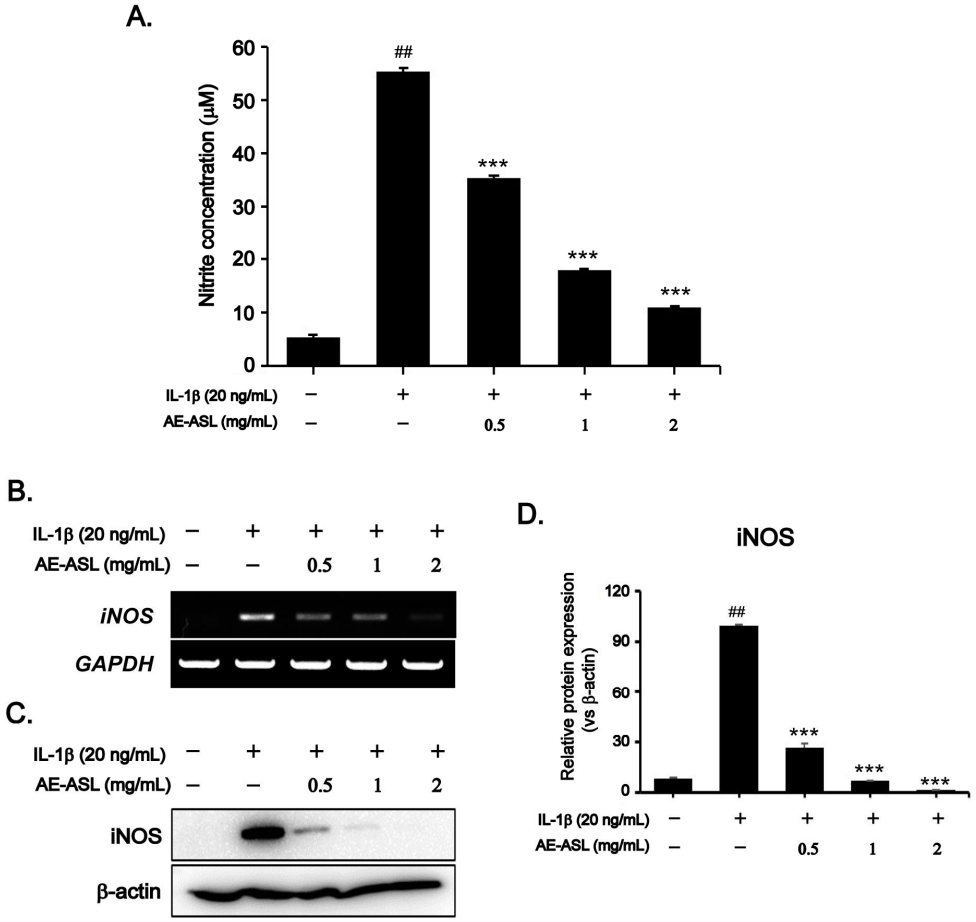

Figure 9. Inhibitory effects of AE-ASL on IL-1β-induced nitirte production and iNOS expression in rat primary chondrocytes. Cells were pretreated with AE-ASL (0.5, 1, and 2 mg/mL) for 1 h, followed by IL-1β (20 ng/mL) stimulation for 24 h. (A) Nitrite production was determined in conditioned medium using Griess reagent after 24 h. (B and C) Expression of iNOS mRNA and protein was determined using RT–PCR and western blot analysis, respectively. (D) Quantitative data of (C) were analyzed using ImageJ software. *GAPDH* and β -actin served as internal controls, respectively. Results are the means ± SD of three independent experiments. ##$P < .01$ compared to the control group; ***$p < 0.001$ compared to the IL-1β-treated group.

4.3. AE-ASL inhibited PGE_2 production and COX-2 expression in IL-1β-stimulated rat primary chondrocytes

To evaluate the effect of AE-ASL on IL-1β-induced PGE_2 production, the accumulation of PGE_2 in the culture supernatant was evaluated using ELISA kit. As shown in Figure 10A, IL-1β alone significantly promoted the generation and release of PGE_2 into the supernatant by 2-fold (942.26 ± 24.50 pg/mL) compared with that in the control (2,045.71 ± 21.95 pg/mL). However, pretreated with AE-ASL for 1 h inhibited IL-1β-induced PGE_2 production in a dose-dependent manner, by 8% (1,888.43 ± 5.09 pg/mL), 16% (1,728.2 ± 4.45 pg/mL), and 30% (1,453.26 ± 8.90 pg/mL) at 0.5, 1, and 2 μg/mL, respectively (Figure 10B). In addition, IL-1β alone significantly increased both the mRNA and protein expression levels of COX-2. However, pretreatment with AE-ASL for 1 h inhibited the IL-1β-induced mRNA and protein expression of COX-2 in a dose-dependent manner (Figure 10B-D). Taken together, these data suggest that the AE-ASL-mediated inhibition of PGE_2 production was associated with the regulation of COX-2 expression in IL-1β-stimulated rat primary chondrocytes.

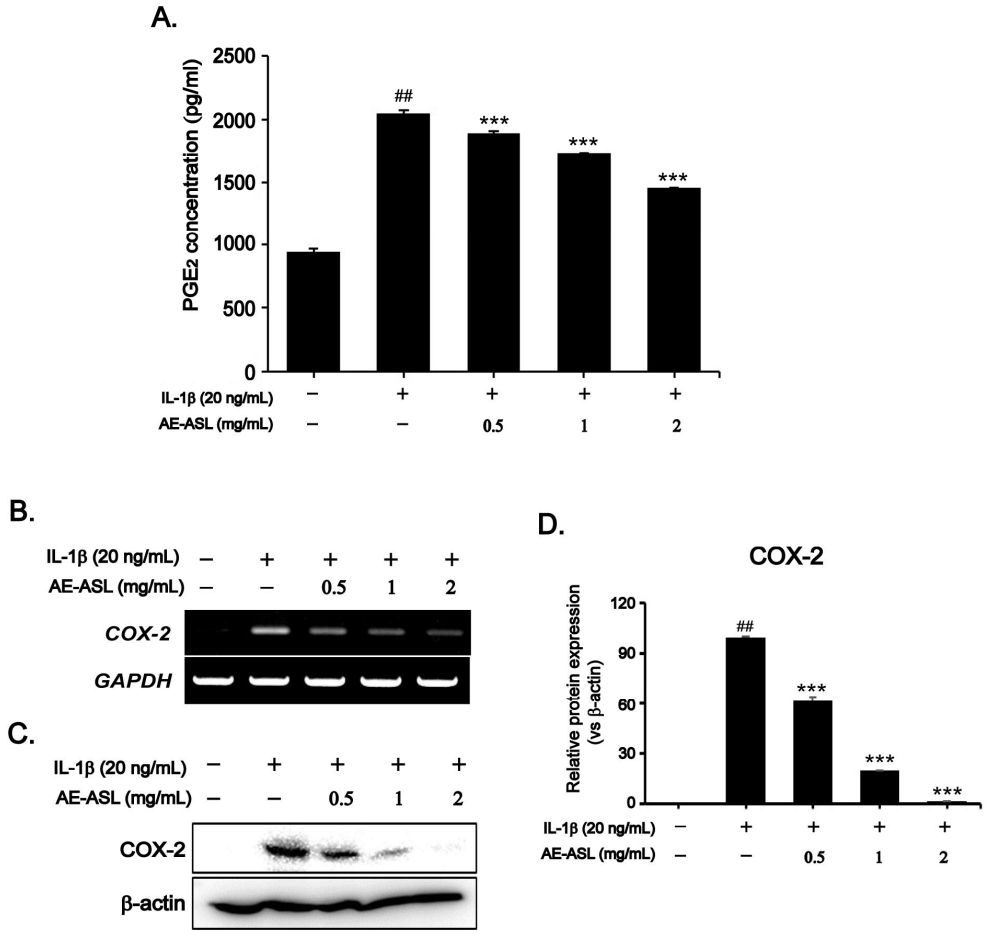

Figure 10. Inhibitory effects of AE-ASL on IL-1β-induced PGE_2 production and COX-2 expression in rat primary chondrocytes. Cells were pretreated with AE-ASL (0.5, 1, and 2 mg/mL) for 1 h, followed by IL-1β (20 ng/mL) stimulation for 24 h. (A) PGE_2 production was determined in the cell culture supernatant using an ELISA kit after 24 h. (B and C) Expression of the COX-2 mRNA and protein was determined using RT-PCR and western blot analysis. (D) Quantitative data of (C) were analyzed using ImageJ software. *GAPDH* and β -actin served as internal controls, respectively. Results are the means ± SD of three independent experiments. ANOVA and Dunnett test were used to evaluate the significance of the results. Results are the means ± SD of three independent experiments. ##$p < 0.01$ compared to the control group; ***$p < 0.001$ compared to the IL-1β-treated group.

4.4. AE-ASL inhibited MMP-3, MMP-13, and ADAMTS-4 expression in IL-1β-stimulated rat primary chondrocytes

Matrix degradation by activation of matrix degrading enzyme such as MMPs and aggrecanase is a representative feature of osteoarthritis [7]. Therefore, the effect of AE-ASL on the IL-1β-induced expression of MMP-3, MMP-13, and ADAMTS-4 was evaluated in rat primary chondrocytes. As shown in Figure 11A and B, IL-1β significantly up-regulated the mRNA and protein expression levels of MMP-3 and MMP-13, whereas pretreatment with the AE-ASL resulted in significant inhibition of IL-1β-induction of these enzyme at both mRNA and protein levels. Moreover, in casein zymography performed to verify the secreted MMP-3 and MMP-13 activity in cultured media, the casein proteolytic activity of these enzymes was significantly increased by IL-1β, but was inhibited by AE-ASL pretreatment dose-dependently in rat primary chondrocytes (Figure 11C). In addition, pretreatment with AE-ASL inhibited the protein expression of IL-1β -induced ADAMTS-4, which is an aggrecanase (Figure 11D). These results suggest that AE-ASL reduced the IL-1β-induced expression of matrix degrading enzymes.

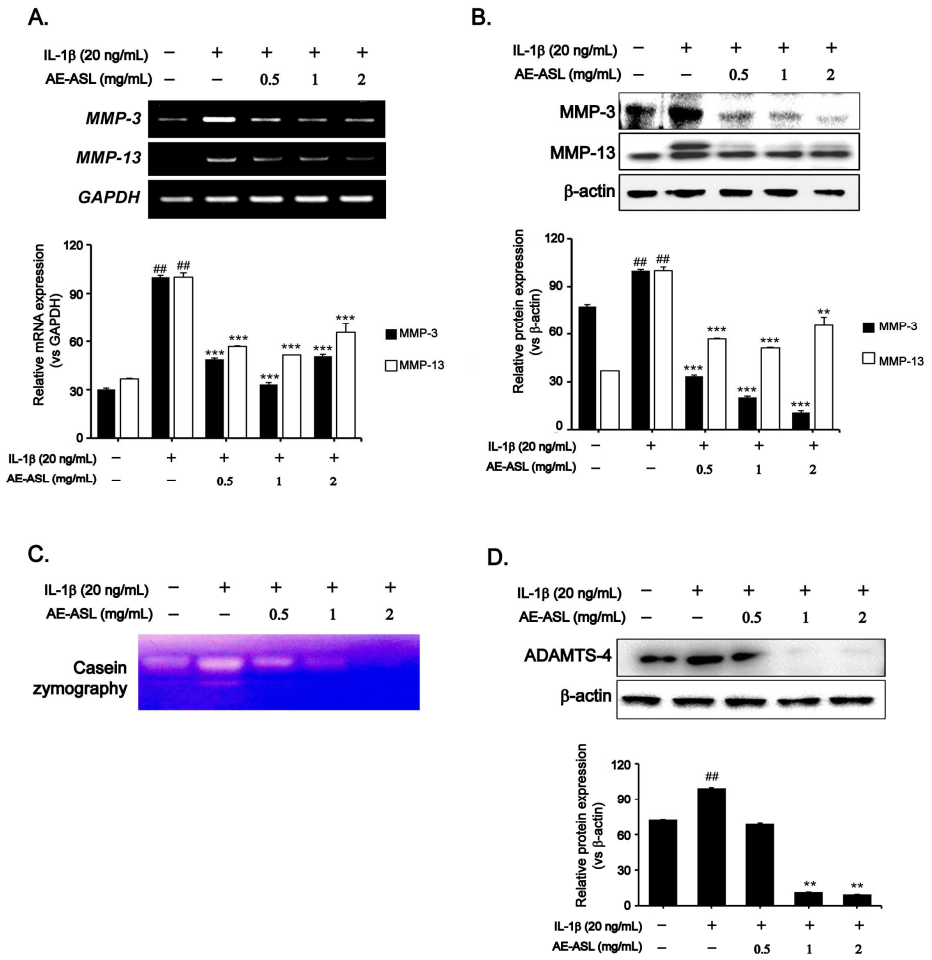

Figure 11. Inhibitory effects of AE-ASL on IL-1β-induced expression of MMP-3, MMP-13, and ADAMTS-4 in rat primary chondrocytes. Cells were pre-treated with 0.5, 1, and 2 mg/mL of AE-ASL for 1 h, followed by IL-1β (20 ng/mL) for 24 h. (A and B) Expression of MMP-3 and MMP-13 mRNA and protein level was determined using RT-PCR and western blot analysis, respectively. (C) Activity of MMPs was measured in conditioned medium using casein zymography. (D) Expression of ADAMTS-4 protein level was determined using western blot analysis. *GAPDH* and β-actin served as internal controls. Quantitative data was analyzed by using ImageJ software. Results are the means ± SD of three independent experiments. ANOVA and Dunnett test were used to evaluate the significance of the results. ##$p < 0.01$ compared with control group; **$p < 0.01$, ***$p < 0.001$ compared with IL-1β-treated group.

4.5. AE-ASL protected degaradation of aggrecan, COL2A1, and proteoglycan in IL-1β-stimulated rat primary chondrocytes

To evaluate whether AE-ASL affects the sGAG contents and expression of aggrecan and COL2A1, which are ECM major components [7], in IL-1β -stimulated rat primary chondrocytes, aggrecan and COL2A1 were detected by ELISA assay, and sGAG contents were detected by DMMB assay. As shown in Figure 12A and B, aggrecan and COL2A1 were significantly decreased by IL-1β, whereas pretreatment with AE-ASL blocked the IL-1β-induced decrease in expression of aggrecan and COL2A1. In addition, the IL-1β-induced release of sGAG was significantly inhibited by pretreatment with AE-ASL (Figure 12C). These results suggest that AE-ASL could be a potent cartilage chondroprotectant by suppressing IL-1β-induced degradation of aggrecan and COL2A1 and release of sGAG in rat primary chondrocytes.

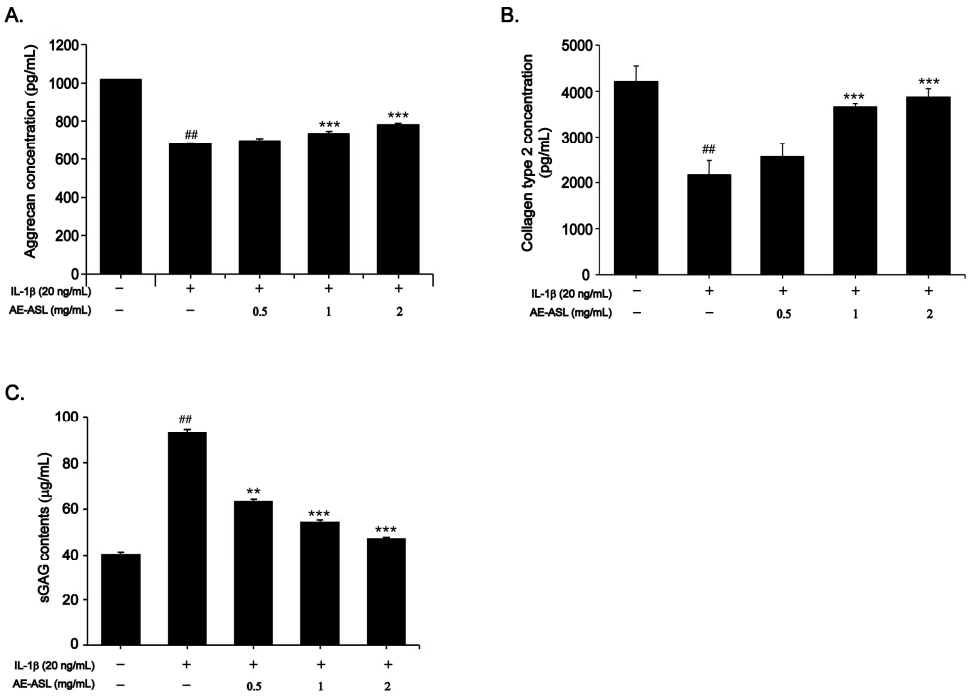

Figure 12. Effect of AE-ASL on IL-1β-induced aggrecan, COL2A1, and proteoglycan degradation in rat primary chondrocytes. Cells were pre-treated with 0.5, 1, and 2 mg/mL of AE-ASL for 1 h, followed by IL-1β (20 ng/mL) for 24 h. Conditioned medium were prepared for aggrecan ELISA assay (A) and COL2A1 ELISA assay (B). (C) The sGAG was measured in conditioned medium using a DMMB assay. Results are the means ± SD of three independent experiments. ANOVA and Dunnett test were used to evaluate the significance of the results. ##P < .01 compared with control group; **p < 0.01, ***p < 0.001 compared with IL-1β-treated group.

4.6. Suppression of NF-κB signaling pathway by AE-ASL in IL-1β -induced rat primary chondrocytes

NF-κB is also an important transcription factor that regulates the transcription of MMPs, ADAMTS family, and inflammatory mediators. Therefore, the effect of AE-ASL on IL-1β-induced NF-κB activation was evaluated in rat primary chondrocytes using western blot analysis. As shown in Figure 13, IL-1β -stimulation for 30 min enhanced the translocation of NF-κB p65 subunit from the cytoplasm to the nucleus, concomitantly with the phosphorylation and degradation of IκBα in the cytoplasm. However, pretreatment with AE-ASL for 1 h suppressed the IL-1β-induced nuclear accumulation of NF-κB p65 subunit and the phosphorylation and degradation of IκBα (Figure 13). These results suggest that AE-ASL inhibited IL-1β-induced NF-κB activation through preventing the nuclear accumulation of NF-κB p65 subunit, and suppression of IκBα phosphorylation and degradation.

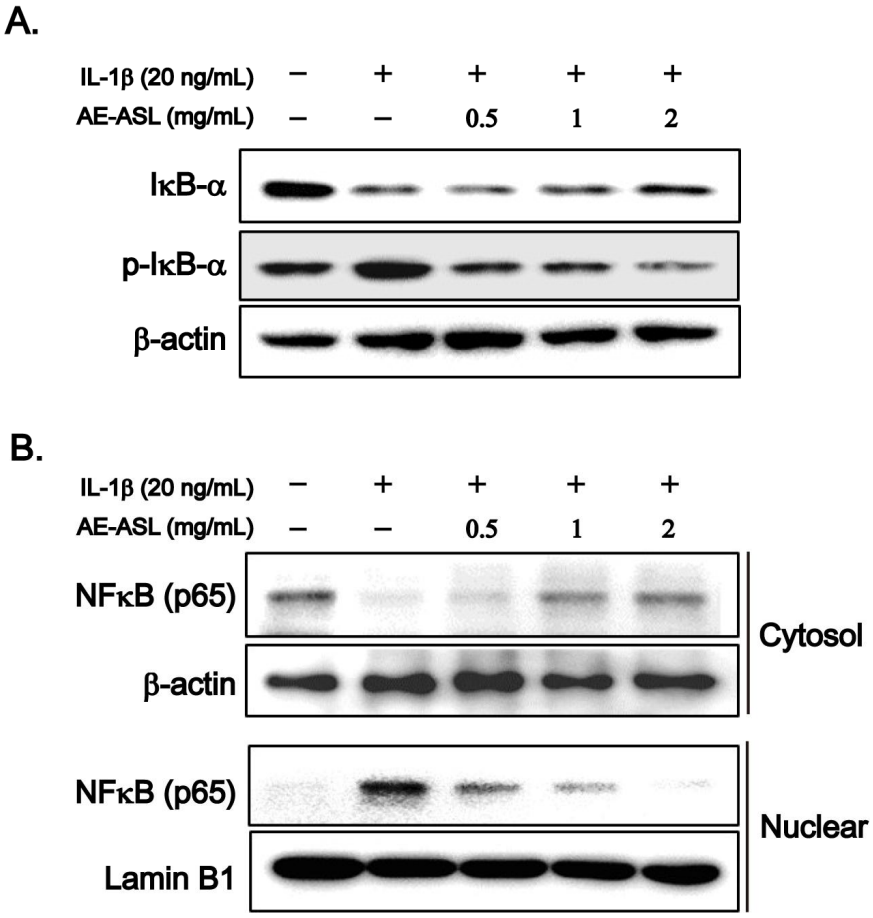

Figure 13. Effects of AE-ASL on IL-1β-induced phosphorylation of IκBα and NF-κB p65 nuclear translocation in rat primary chondrocytes. Cells were pre-treated with 0.5, 1, and 2 mg/mL of AE-ASL for 1 h, followed by IL-1β (20 ng/mL) for 1 h. (A) Protein levels of IκB-α and phosphorylated IκB-α were determined using western blot analysis. (B) Protein levels of NF-κB p65 in nuclear and cytosolic extracts were determined using western blotting. β-actin and lamin B1 were used as cytosolic and nuclear internal controls, respectively.

4.7. AE-ASL inhibited phosphorylation of MAPKs in IL-1β-stimulated rat primary chondrocytes

As it is well known that IL-1β-induced MMPs expression is mediated by activation of the family of MAPK kinases including ERK, JNK, and p38 MAPK. Therefore, it was evaluated whether AE-ASL exhibited the inhibitory effect of catabolic factors through these kinases. Chondrocytes stimulated with IL-1β activated the phosphorylation of ERK, JNK, and p38 MAPK, without markedly affecting their total protein levels (Figure 14A and B). However, pretreatment with AE-ASL inhibited the IL-1β-induced phosphorylation of ERK, JNK, and p38 MAPK to near the control levels. These results suggest that the suppressive effect of AE-ASL on IL-1β-induced expression of cartilage degrading enzymes was mediated through MAPK signaling in rat primary chondrocytes.

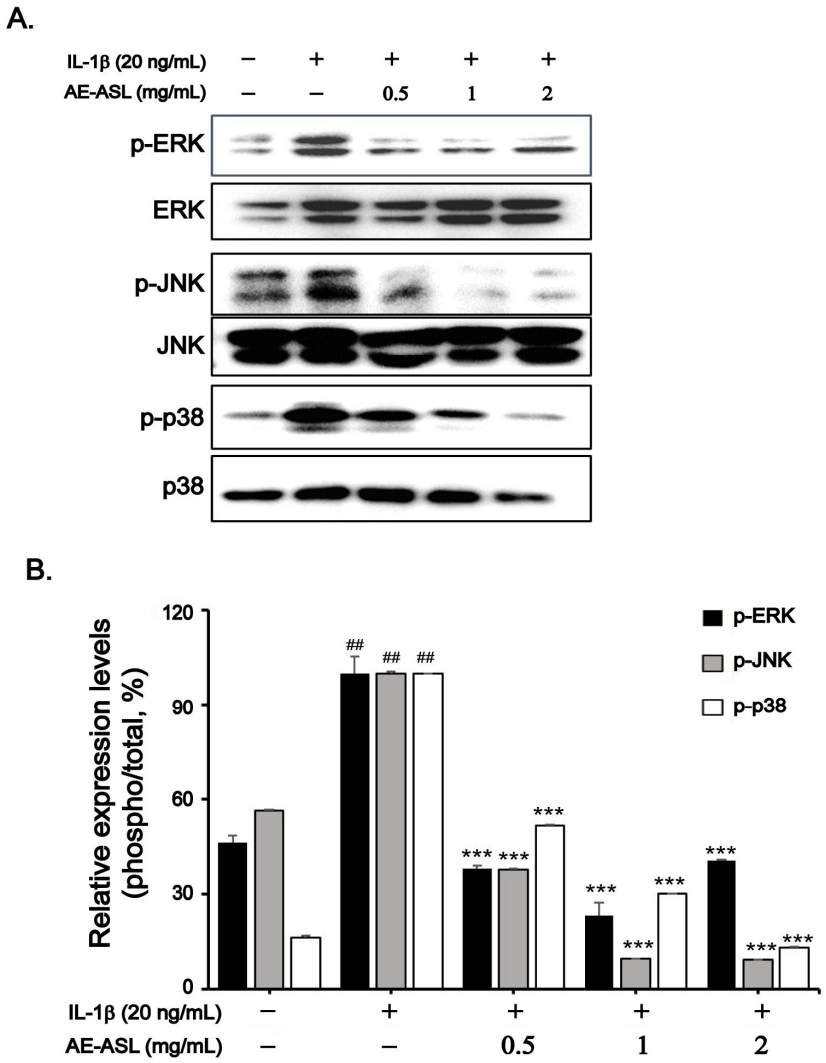

Figure 14. Effects of AE-ASL on IL-1β-induced phosphorylation of ERK, JNK, and p38 in rat primary chondrocytes.

Cells were pre-treated with 0.5, 1, and 2 mg/mL of AE-ASL for 1 h, followed by IL-1β (20 ng/mL) for 1 h. (A) Total and phosphorylated ERK, JNK, and p38 were determined using western blotting. (B) Quantitative data of (A) were analyzed using ImageJ software. Results are the means ± SD of three independent experiments. ANOVA and Dunnett test were used to evaluate the significance of the results. ##p < 0.01 compared with control group; ***p < 0.001 compared with IL-1β-treated group.

4.8 Effect of AE-ASL administration on macroscopic and histologic parameters in articular cartilage of OA rat model

The preventive efficacy of AE-ASL on DMM-induced OA was evaluated by assessing the structural integrity of the articular cartilage using microscopic observation of cartilage surfaces, Safranin-O/Fast green staining, and an OARSI score. As shown in Figure 15A and B, the articular cartilage in OA group with an OARSI score of 11 ± 0.5 exhibited proteoglycan depletion, cartilage superficial destruction, and cartilage erosion, indicating moderate pathological osteoarthritic compared with the control and sham group. However, the 50, 100, and 200 mg/kg of AE-ASL-treated OA groups showed less proteoglycan loss and cartilage destruction, with a significantly lower OARSI score (7.5 ± 0.28, 6.0 ± 0.5, and 3.5 ± 0.28, respectively) (Figure 15A and B). On the cartilage surface macroscope observation, cartilage defects were found in the tibia and femur cartilage surface of the OA group, but defects were not seen in the AE-ASL-treated OA group (Figure 15C). Taken together, these results suggest that AE-ASL attenuated the progression of OA in rat OA model.

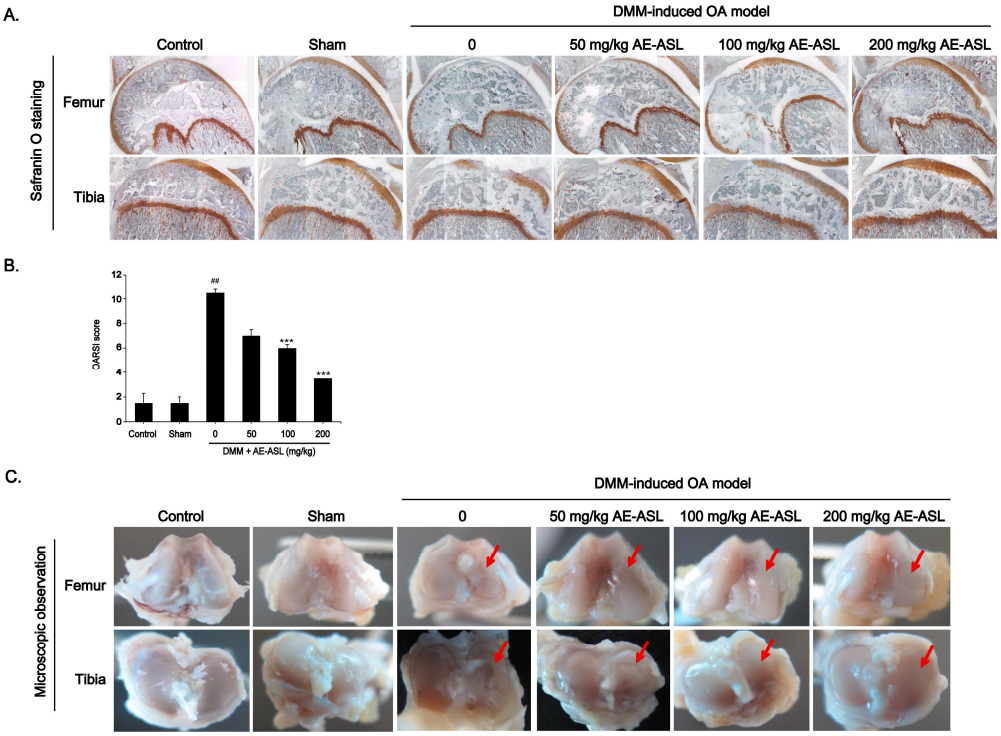

Figure 15. Histological evaluation and microscopic observation of cartilage-protective effect of AE-ASL against cartilage degradation in DMM-induced OA rat models. After sham or DMM surgery, rats received a gavage of distilled water or AE-ASL (50, 100, and 200 mg/kg bodyweight) daily for 8 weeks. Histological analysis of cartilage destruction was evaluated by safranin O/fast green staining (A) and Osteoarthritis Research Society International (OARSI) advanced Osteoarthritis Cartilage Histopathology Assessment System (B). (C) Macroscopic observation exhibits representative each group. ANOVA and Dunnett test were used to evaluate the significance of the results. ##$p < 0.01$ compared with sham group; ***$p < 0.001$ compared with DMM group.

5. Identification of AE-ASL and evaluation of anti-osteoarthritic efficacy *in vitro*

5.1. Components identification of AE-ASL

The major components of the extract were separated and analyzed using preparative HPLC, and three components with retention time of 8.47 min, 11.46 min, and 12.60 min were detected at 320 nm wavelength (Figure 16A). The mass spectrometric analysis of these fraction was performed by HPLC-ESI-TOF/MS under the same conditions, as a result, each peak with retention time of 4.75 min, 7.20 min and 8.01 min was detected at 320 nm wavelength (data not shown). As shown Figure 16B, compound 1 is predicted to be a chlorogenic acid having a M.W. of 354.0951 and a formula of $C_{16}H_{18}O_9$, and compound 2 having a M.W. of 48.1006 and formula of $C_{21}H_{20}O_{11}$ is shown as a cynaroside, and compound 3 having a M.W. of 534.1010 and formula of $C_{24}H_{22}O_{14}$ is expected to be luteolin-7-O-malonylgluces.

A.

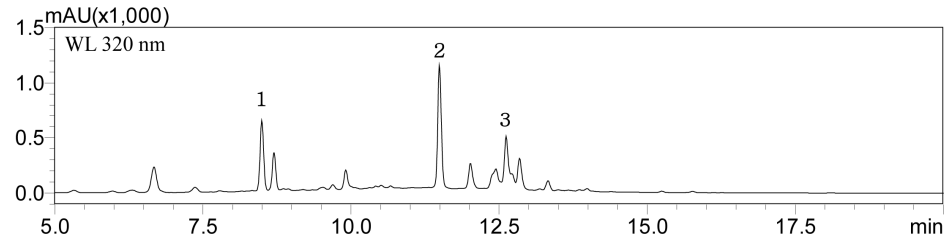

B.

Compound #	R.T. (min)	λmax	ESI-TOF-MS(m/z)		Predicted M.W. (g ·mol^{-1})	Predicted M.F.	Candidate Compound
			Molecular ion	Fragment ion			
1	4.75	326	355.0987 $[M+H]^+$	163.039 $[M\text{-qunic}]^+$	354.0951	$C_{16}H_{18}O_9$	**Chlorogenic acid**
2	7.20	254, 348	449.1052 $[M+H]^+$	287.0550 $[M\text{-Glu}]^+$	448.1006	$C_{21}H_{20}O_{11}$	**Cynaroside**
3	8.01	254, 348	535.1047 $[M+H]^+$	287.0550 $[M\text{-Glu-malonly}]^+$	534.1010	$C_{24}H_{22}O_{14}$	**Luteolin-7-O-malonylglucose**

Figure 16. Components identification of AE-ASL. (A) The analytical HPLC chromatograms of raw material of AE-ASL. (B) HPLC-ESI-TOF/MS accurate mass measurements of the three main phenolic compounds in the AE-ASL.

5.2. Screening of active components of AE-ASL *in vitro*

To examine the potential anti-inflammatory properties of AE-ASL components, the effects of three components, chlorogenic acid, cynaroside (luteolin-7-O-glucoside), and luteolin-7-O-malonylglucoside, on the inhibition of nitrite production following stimulation with LPS was evaluated in RAW264.7 cells. Treatment of RAW264.7 with LPS alone significantly increased the nitrite production by 13-fold (13.60 ± 0.38 uM), whereas pretreatment with 3 components inhibited the LPS-induced nitrite production. Of the three components, cynaroside had the highest inhibitory effect on nitrite production, and inhibition rates were 31% (9.13 ± 0.19 uM), 40% (7.84 ± 0.1 uM), 47% (6.90 ± 0.29 uM) and 50% (6.56 ± 0.19 uM) at 5, 10, 20, and 40 uM, respectively (Figure 17). Therefore, it was analyzed the contents of cynaroside contained in AE-ASL, and found that 20 mg of cynaroside was contained per 1 g of extract powder. To confirm that cynaroside is a component that can be responsible for the chondroprotective effect of AE-ASL, the inhibitory effects of cynaroside and AE-ASL were compared to the nitric oxide production by IL-1β in rat primary chondrocytes. The cells were pretreated with AE-ASL (0.5, 1, and 2 mg/mL) or cynaroside (10, 20, and 40 μg/mL) for 1 h, and then subsequently cultured with IL-1β (20 ng/mL) for 24 h. As shown in Figure 18, the effect of cynaroside was comparable to that of AE-ASL, and these results suggest that cynaroside may be a representative component of AE-ASL.

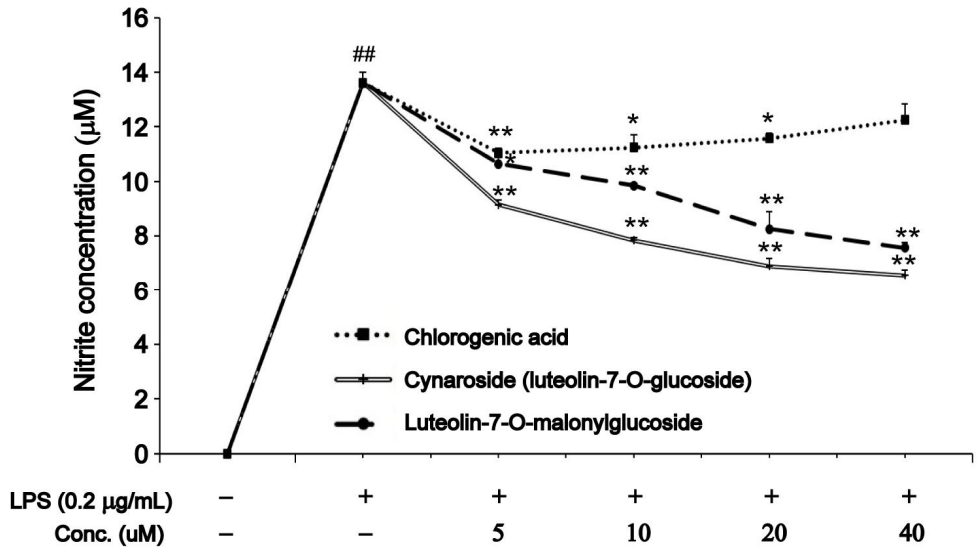

Figure 17. Screening of active components of AE-ASL. RAW2647 cells were pretreated with 3 components (5, 10, 20, and 40 μM) for 1 h, followed by LPS (0.2 μg/mL) stimulation for 24 h**.** Nitrite production was determined in the cell culture supernatant using the Griess reagent. Results are the means ± SD of three independent experiments. ##p < 0.01 compared to the control group; *p < 0.05, **p < 0.01 compared to the LPS-treated group.

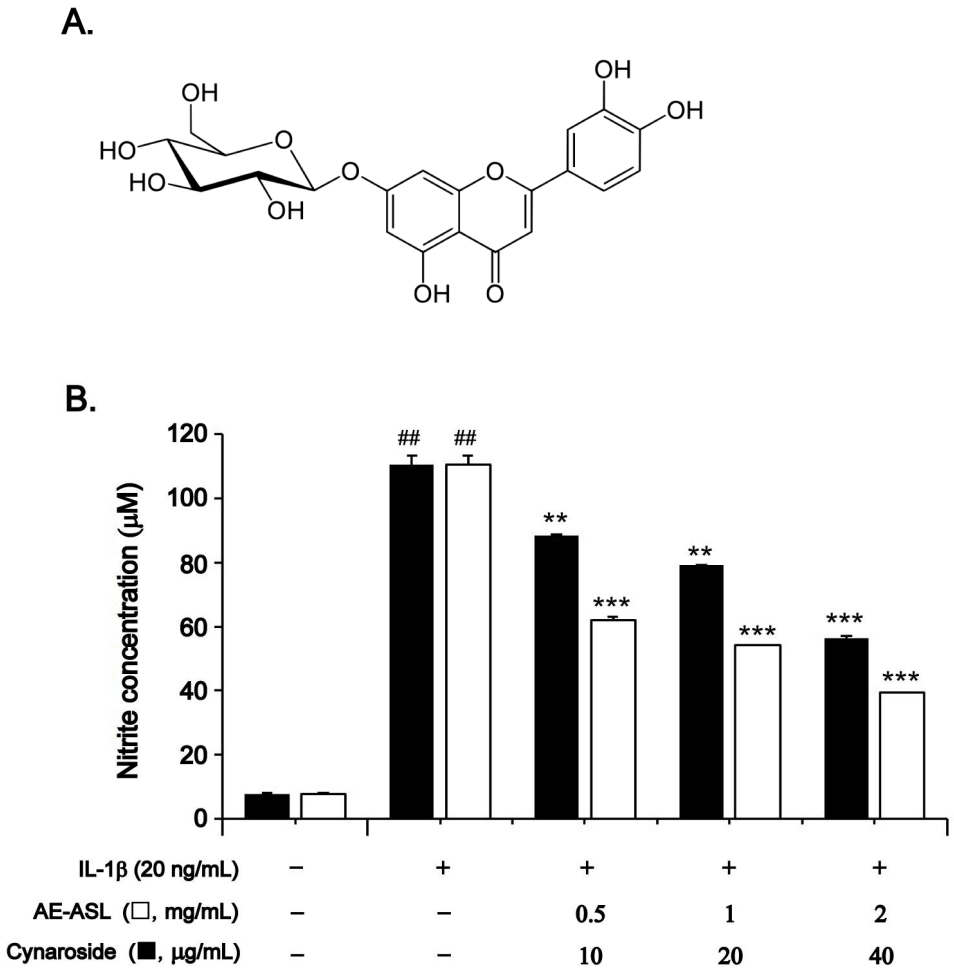

Figure 18. Inhibitory effects of AE-ASL and cynaroside on IL-1β-induced nitirte production in rat primary chondrocytes.

Cells were pretreated with cynaroside (10, 20, and 40 μg/mL) or AE-ASL (0.5, 1, and 2 mg/mL) for 1 h, followed by IL-1β (20 ng/mL) stimulation for 24 h. (A) Structure of cynaroside (luteolin-7-O-glucoside) (B) Nitrite production was determined in conditioned medium using Griess reagent after 24 h. Results are the means ± SD of three independent experiments. ##$p < 0.01$ compared to the control group; **$p < 0.01$, ***$p < 0.001$ compared to the IL-1β-treated group.

5.3 Cynaroside represents the anti-osteoarthritic effect of AE-ASL in rat primary chondrocytes

It was evaluated whether cynaroside contributed to the observed effects of AE-ASL on expression of catabolic or anabolic factors in rat primary chondrocytes. As shown in Figure 19, cynaroside suppressed IL-1β-induced expression of catabolic factors, iNOS, COX-2, TNF-α, MMP-13, and ADAMTS-4 (Figure 19A and B), whereas protected IL-1β-induced decrease of anabolic factors, aggrecan (Figure 19C). In addition, the chondroprotective effect of cynaroside was confirmed by alcian blue staining, which stained GAG of cartilage. As shown in Figure 19D, the IL-1β treated group showed a slightly cloudy staining compared to the control group, whereas that in the group pretreated with cynaroside (40 μg/mL) showed a higher degree of staining. These result suggest that cynaroside contributes to the chondroprotective effect of AE-ASL.

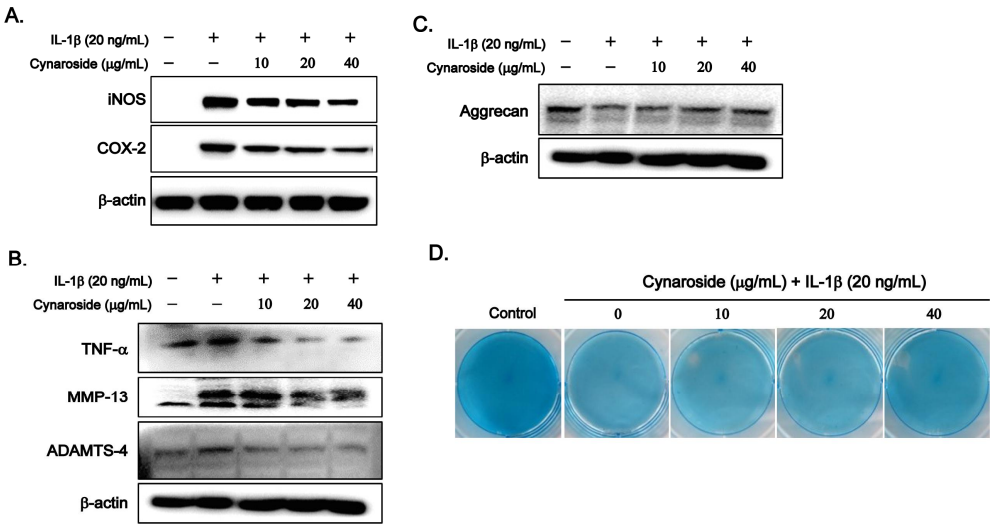

Figure 19. Anti-osteoarthritic effects of cynaroside in IL-1β-stimulated rat primary chondrocytes. Cells were pretreated with cynaroside (10, 20, and 40 μg/mL) for 1 h, followed by IL-1β (20 ng/mL) stimulation for 24 h. (A and B) Protein expression level of the catabolic factors, iNOS, COX-2, TNF-α, MMP-13, and ADAMTS-4, was measured using western blot analysis, respectively. (C) Protein expression level of the anabolic factor, aggrecan. (D) Alcian blue staining for analysis of GAG accumulation.

Ⅳ. Discussion

Anthriscus sylvestris is a medicinal plant that has long been used as traditional medicine in Korean and other countries [27-29]. It has been reported that aerial parts show antioxidant effects, whereas dried roots show antitumor activity by inducing the cell cycle arrest and apoptosis *in vitro* and *in vivo* [27,31,32,39] However, physiologically active functions of aqueous extract of *A. sylvestris* leaves (AE-ASL) are not yet known. Therefore, in this study, anti-inflammatory effect and chondroprotective effect of AE-ASL was investigated. In firth first section, anti-inflammatory effects of AE-ASL was evaluated *in vitro* in LPS-stimulated RAW264.7 cells and *in vivo* in a carrageenan-induced paw edema animal model. Furthermore, based on these anti-inflammatory effect, in the second section, chondroprotective effect against inflammation of AE-ASL was evaluated *in vitro* in rat primary chondrocytes, and its effects were demonstrated *in vivo* in a DMM surgery-induced OA rat model.

Macrophages, differentiated from monocytes, play a pivotal role in many diseases, including infection, inflammation, atherosclerosis, and cancer [40]. Macrophages activated by external stimuli, such as LPS and IFN-γ, induce inflammation via the excessive secretion of cytokines and inflammatory mediators such as TNF-α, IL-1β, iNOS, and PGE_2 [40]. IL-1β is a major pro-inflammatory cytokine that initiates and enhances the inflammatory response, and IL-6 is also crucially involved in the acute-phase of the immune response [41,42]. In addition, TNF-α is one of the major upstream cytokines that can activate the NF-κB pathway, and stimulate the release of other pro-inflammatory cytokines such IL-1β and IL-6 [42,43]. Furthermore, metabolites, such as NO and COX-2, of inflammatory mediators, such as iNOS and PGE_2, maintain a constant inflammatory environment, and cytokines function as chemokines for increasing the macrophage population, leading to an exacerbated inflammation [44,45]. Therefore, inhibiting the expression of these inflammation-related genes in

activated macrophages can be an attractive strategy for the development of anti-inflammatory drugs, and many studies have demonstrated the anti-inflammatory efficacy of natural products by assessing the inhibition of the expression of these genes [46-49]. Results showed that AE-ASL significantly inhibited the LPS-induced NO and PGE_2 production by suppressing iNOS and COX-2 mRNA and protein expression in activated macrophages (Figure 2 and 3). In addition, pretreatment with AE-ASL decreased the expression of LPS-induced proinflammatory cytokines, TNF-α, IL-1β, and IL-6, in dose-dependent manners (Figure 4). These findings are consistent with the results of other reports, which investigated the anti-inflammatory effects of various plant extracts, [50-52] and support our hypothesis that AE-ASL has anti-inflammatory activity.

To further clarify the anti-inflammatory mechanism of AE-ASL, its effects on the activation of the NF-κB and MAPK signaling pathways were evaluated in LPS-stimulated macrophages. These signaling pathways are well known to regulate the expression of numerous genes associated with the immunity, such as those encoding iNOS, COX-2, TNF-α, IL-1β, and IL-6 [37,38]. Results showed that pretreatment with AE-ASL suppressed the translocation of the NF-κB p65 subunit from the cytoplasm to the nucleus via inhibition of the LPS-induced phosphorylation and degradation of IκB-α (Figure 5). In addition, pretreatment with AE-ASL inhibited the LPS-induced phosphorylation of ERK, JNK, and p38 MAPK (Figure 6). These data indicate that the NF-κB and MAPK signaling pathways may mediate the inhibition of proinflammatory mediators and cytokines by AE-ASL in LPS-stimulated RAW264.7 cells, which agrees with the data from previous studies of other researchers [48-52].

Carrageenan is a strong stimulant of proinflammatory mediators and the inflammatory responses induced by carrageenan occur as a biphasic process [53]. The early phase (2 h after carrageenan injection) is mainly mediated by the release of histamine and serotonin, while the late phase (the first 3–4 h) is

mediated by the release of bradykinin, TNF-α, and leukotrienes and is sustained by PGE_2 and COX-2 [53,54]. Thus, most conventional anti-inflammatory drugs target the late phase [55]. *In vivo* study showed that orally administered AE-ASL inhibited the carrageenan-induced paw edema in a dose-dependent manner for up to 4 h after the carrageenan injection, and 200 mg/kg AE-ASL was especially effective in the early phase of the carrageenan-induced inflammatory response (Figure 7). These anti-inflammatory properties of AE-ASL have potential as therapeutic agents for various diseases caused by inflammation and can positively affect the improvement of osteoarthritis caused by inflammation.

OA is a disease commonly seen in the elderly, due to cartilage wearing out through the long-term use of joints and inflammation [1,2]. Cartilage wear is promoted mainly by the degradation of cartilage matrix by the inflammatory responses caused by friction between the cartilaginous tissues. OA rapidly progresses through vicious circle of inflammation and catabolism [1,2]. Therefore, most drugs for treating OA including acetaminophen, duloxetine, and NSAIDs, are aimed at treating inflammation and inhibiting inflammation-induced pain [56]. However, long-term use of these drugs exhibits severe side effects such as gastrointestinal and renal toxicity [56]. Thus, it is very important to develop OA drugs with fewer side effects, because OA is a very common disease in elderly population.

Inflammation affecting the catabolism of cartilage is a strong inducer of OA pathogenesis, and chondrocyte apoptosis by inflammation markedly reduces the tissue maintenance and functionality, further restraining the regeneration ability of joint [3,57]. In particular, IL-1β by inflammation releases cartilage-degrading enzymes such as MMPs, ADAMTS family, and other catabolic enzymes, and, consequently, cartilage matrix degradation promotes OA pathogenesis [5]. Several studies reported that inhibition of IL-1β-induced inflammation mediators such as NO and PGE_2 had the ability to alleviate OA pathogenesis, reduce pain, inflammation, and proteoglycan loss [3,6]. Therefore, inhibition of these

inflammatory mediators is a greatly effective therapeutic target for OA treatment. Results showed that AE-ASL inhibited IL-1β-induced nitrite, iNOS, PGE_2, and COX-2 expression in a dose-dependent manner, which suggested that AE-ASL has a potent anti-inflammation activity on IL-1β-stimulated rat primary chondrocytes.

MMPs are a family of proteolytic enzymes and are over-released in cartilage tissues and synovial fluid to trigger OA, by degrading ECM [7]. In particular, MMP-3 and MMP-13 decompose aggrecan and COL2A1, which are ECM major components, and this decomposition product stimulate synoviocytes and provide a suitable microenvironment for the progression of OA through a vicious circle that induces inflammation [7]. In addition, aggrecan degradation induces the release of sGAG, which plays an important role in cartilage elasticity by binding to the aggrecan core protein to form proteoglycans. ADAMTS-4 is considered the primary enzyme responsible for the degradation of aggrecan in OA pathogenesis [13,58]. Therefore, the contents of cartilage matrix factors, such as aggrecan, COL2A1 and proteoglycan, were considered as a crucial parameter to assess progression of the cartilage destruction. Results showed that AE-ASL inhibited the IL-1β-induced production of MMP-3, MMP-13, and ADAMTS-4 in rat primary chondrocytes (Figure 11). In addition, pretreatment with AE-ASL suppressed the IL-1β-induced decreased aggrecan and COL2A1 protein level (Figure 12). Furthermore, consistent with the inhibitory effect of AE-ASL on decreased aggrecan and COL2A1 by IL-1β, AE-ASL suppressed the increase in IL-1β -induced sGAG contents to near normal levels.

IL-1β exhibits its effects on the expression of MMPs, COX-2, iNOS by mainly activating MAPKs and the NF-κB signaling pathway [59,60]. Several studies reported that inhibition of MAPKs (ERK1/2, JNK, and p38 MAPK) phosphorylation and NF-κB p65 subunit translocation to the nucleus pathways resulted in the inhibition of IL-1β-induced expression of MMPs, COX-2, iNOS, and pro-inflammation cytokines in rabbit chondrocytes [20,61]. Therefore, the

effects of AE-ASL on the IL-1β-induced phosphorylation of MAPKs and NF-κB p65 subunit translocation was evaluated. Pretreatment with AE-ASL suppressed the phosphorylation of MAPKs and translocation of the NF-κB p65 subunit to the nucleus in IL-1β-induced rat primary chondrocytes (Figure 13 and 14).

Furthermore, to verify whether AE-ASL has a chondroprotective effect, the cartilage destruction and changes were evaluated in DMM surgery-induced OA rat model. This model has been widely used to assess agents' efficacy because it resembles the OA pathogenesis associated with human aging through incising the meniscus and inducing degeneration [62]. In addition, histological staining after *in vivo* experiments can be provide specific information on physiological and pathological condition in articular cartilage, such as distribution of chondrocytes and matrix components, so it is commonly used to evaluate the effect of improving arthritis [63]. The results of the histological examinations showed that DMM resulted in cartilage degradation, whereas the oral administration of AE-ASL for 8 weeks inhibited cartilage degradation, and this result was consistent with the OARSI score. Furthermore, HPLC and HPLC-ESI-TOF/MS analysis to find the active components responsible for these efficacy of the AE-ASL was evaluated. As a result, phenolic compounds, chlorogenic acid, cynaroside, and luteolin-7-O-malonylglucose were identified (Figure 16). Of these components, cynaroside had the highest inhibitory effect on nitrite production in LPS-stimulated RAW26.7 cells (Figure 17), and showed chondroprotective effect in IL-1β-stimulated rat primary chondrocytes (Figure 18). Dall'Acqua *et al*. reported that chlorogenic acid and cynaroside are the active components with antioxidant activity in the methanol extract of *A.sylvestris* aerial parts [32]. Luteolin-7-O-glucoside (cynaroside) isolated from *A. sylvestris* was confirmed by the work of Zemlicka *et al* as the dominant polyphenolic species and as active components with antioxidant activity [64]. In addition, chlorogenic acid and cynaroside were reported to exert anti-inflammatory effects in mice with D-gal-induced chronic liver injury and

in a carrageenan-induced paw edema rat model [65,66]. These results suggest strongly imply that the these observed effect of AE-ASL could be attributed to the effect of its predominant component cynaroside.

Collectively, anti-inflammatory effect *in vitro* data showed that AE-ASL suppressed LPS-induced expression of inflammatory-related factors, such as nitrite, iNOS, PGE_2, COX-2 and pro-inflammatory cytokines by suppressing NF-κB activity and the MAPK signaling pathway in RAW264.7 cells. In addition, anti-inflammatory *in vivo* data showed that oral administration with AE-ASL inhibited the carrageenan-induced paw edema in a dose-dependent manner for up to 4 h after the carrageenan injection. Chondroprotective effect *in vitr*o data showed that AE-ASL suppressed the IL-1β-induced expression of inflammatory-related factors, such as nitrite, iNOS, PGE_2, COX-2, and cartilage-degrading enzymes, such as MMP-3, MMP-13 and ADAMTS-4, by suppressing NF-κB activity and the MAPK signaling pathway in rat primary chondrocytes. Furthermore, AE-ASL protected IL-1β-induced decreased expression of anabolic factors, aggrecan, COL2A1 and proteoglycan *in vitro*. In addition, chondroprotective effect *in viv*o data showed that oral administration with AE-ASL decreased DMM surgery-induced matrix loss and cartilage degeneration. Overall, these results suggest that AE-ASL has the possibility of development as a preventive and therapeutic agent for osteoarthritis. However, although the evaluation of the efficacy of osteoarthritis and its mechanism studies can be done with a single osteoarthritis model, there are limitations that do not reflect all aspects of human disease. Therefore, in order to clarify the effect of AE-ASL improvement on degenerative arthritis, long-term studies *in vitro* and *in vivo* are required not only for small animals but also large-scale animals.

Ⅴ. Conclusion

Osteoarthritis (OA) is a degenerative disease commonly occurring in the elderly, accompanied by deformation of articular cartilage, subchondral bone remodeling, osteophyte formation and pain. *Anthriscus sylvestris* is a medicinal plant that has long been used as traditional medicine in Korean and other countries. However, physiological functions of aqueous extract of AE-ASL are not yet well known. Therefore, in this study, the chondroprotective effects of AE-ASL was evaluated.

Anti-inflammatory efficacy on LPS-stimulated mouse marcophage RAW264.7 cells,

1. Pretreatment with AE-ASL inhibited production and expression of inflammatory mediators and cytokines, including nitrite, PGE_2, iNOS, COX-2, TNF-α, IL-1β, and IL-6 in dose-dependent manners.
2. Pretreatment with AE-ASL suppressed translocation of the NF-κB p65 subunit to the nucleus and phosphorylation of ERK, JNK, and p38 MAPK.
3. *In vivo* study, orally administered AE-ASL inhibited the carrageenan-induced paw edema in a dose-dependent manner for up to 4 h after the carrageenan injection.

Chondroprotective efficacy on IL-1β-stimulated rat primary chondrocytes,

1. Pretreatment with AE-ASL inhibited production and expression of inflammatory mediators and cartilage degrading enzymes, including nitrite, PGE_2, iNOS, COX-2, MMP-3, MMP-13, and ADAMTS-4, but pretreatment with AE-ASL protected the degradation of aggrecan, COL1A1 and proteoglycan.
2. Pretreatment with AE-ASL suppressed translocation of the NF-κB p65 subunit to the nucleus and phosphorylation of ERK, JNK, and p38 MAPK.
3. *In vivo* study, DMM surgery resulted in cartilage degradation, whereas daily oral administration of AE-ASL for 8 weeks inhibited DMM surgery-induced

cartilage degradation.

4. AE-ASL contains phenolic compounds, such as chlorogenic acid, cynaroside, and luteolin-7-O-malonylglucose.
5. The observed chondroprotective effects of AE-ASL could be attributed to the effect of its predominant component cynaroside.

The results of this study show that AE-ASL has a potent anti-inflammatory efficacy and chondroprotective efficacy, suggesting that AE-ASL can be developed as a promising OA preventive and therapeutic agent.

References

1. Van den Berg W.B. Pathophysiology of osteoarthritis. *Joint Bone Spine*. 2000;67(6):555–556.
2. Loeser R.F., Goldring S.R., Scanzello C.R., Goldring M.B. Osteoarthritis: a disease of the joint as an organ. *Arthritis Rheum*. 2012;64(6):1697–1707.
3. Khan N.M., HaseebA., Ansari M.Y., Haqqi T.M. a wogonin-rich-fraction of *Scutellaria baicalensis* root extract exerts chondroprotective effects by suppressing IL-1β-induced activation of AP-1 in human OA chondrocytes. *Sci. Rep*. 2017;7:43789.
4. Libby P. Inflammatory mechanisms: the molecular basis of inflammation and disease. *Nutr Rev* 2007;65:S140–S146.
5. Kobayashi M., Squires G.R., Mousa A., Tanzer M., Zukor D.J., Antoniou J., Feige U., Poole A.R. Role of interleukin-1 and tumor necrosis factor alpha in matrix degradation of human osteoarthritic cartilage. *Arthritis Rheum*. 2005;52(1):128–135.
6. Zheng M., Feng Z., You S., Zhang H., Tao Z., Wang Q,, Chen H., Wu Y. Fisetin inhibits IL-1β-induced inflammatory response in human osteoarthritis chondrocytes through activating SIRT1 and attenuates the progression of osteoarthritis in mice. *Int. Immunopharmacol*. 2017;45:135–147.
7. Burrage P.S., Mix K.S., Brinckerhoff C.E. Matrix metalloproteinases: role in arthritis. *Front. Biosci*. 2006;11(1):529–543.
8. Goldring M.B., Otero M., Plumb D.A., Dragomir C., Favero M., El Hachem K., Hashimoto K., Roach H.I., Olivotto E., Borzi R.M., Marcu K.B. Roles of inflammatory and anabolic cytokines in cartilage metabolism: signals and multiple effectors converge upon MMP-13 regulation in osteoarthritis. *Eur. Cell Mater*. 2011;21(24):202–220.
9. Shiomi T., Lemaître V., D'Armiento J., Okada Y. Matrix metalloproteinases, a disintegrin and metalloproteinases, and a disintegrin and metalloproteinases with

thrombospondin motifs in non-neoplastic diseases. *Pathol. Int.* 2010;60:477-496.

10. Wang M.. Sampson E.R., Jin H.T., Li J., Ke Q.H., Im J.H., Chen D. MMP13 is a critical target gene during the progression of osteoarthritis. *Arthritis Res Ther.* 2013;15:R5
11. Roach H.I., Yamada N., Cheung K.S., Tilley S., Clarke N.M., Oreffo R.O., Kokubun S., Bronner F. Association between the abnormal expression of matrix degrading enzymes by human osteoarthritic chondrocytes and demethylation of specific CpG sites in the promoter regions. *Arthritis Rheum.* 2005;52:3110-3124.
12. Neuhold L.A., Killar L., Zhao W., Sung M.L., Warner L., Kulik J., Turner J., Wu W., Billinghurst C., Meijers T., Poole A.R., Babij P., DeGennaro L.J. Postnatal expression in hyaline cartilage of constitutively active human collagenase-3 (MMP-13) induces osteoarthritis in mice. *J. Clin. Invest.* 2001;107:35-44.
13. Majumdar M.K., Askew R., Schelling S., Stedman N., Blanchet T., Hopkins B., Morris E.A., Glasson S.S. Double-knockout of ADAMTS-4 and ADAMTS-5 in mice results in physiologically normal animals and prevents the progression of osteoarthritis. *Arthritis Rheum*. 2007;56(11):3670–3674.
14. Knudson C.B., Knudson W. Cartilage proteoglycans. *Semin. Cell Dev. Biol*. 2001;12(2):69–78.
15. Mevel E., Merceron C., Vinatier C., Krisa S., Richard T., Masson M., Lesoeur J., Hivernaud V., Gauthier O., Abadie J., Nourissat G., Houard X., Wittrant Y., Urban N., Beck L., Guicheux J. Olive and grape seed extract prevents post-traumatic osteoarthritis damages and exhibits i*n vitro* anti IL-1β activities before and after oral consumption. *Sci. Rep.* 2016;6(19):33527.
16. Le Graverand-Gastineau M.P., Disease modifying osteoarthritis drugs: facing development challenges and choosing molecular targets. *Curr. Drug Targets.* 2010;11(5):528–535.
17. Recommendations for the medical management of osteoarthritis of the hip and

knee: 2000 update. American College of Rheumatology Subcommittee on Osteoarthritis Guidelines. *Arthritis Rheum.* 2000;43(9):1905–1915.

18. Burrage N., Haqqi T.M. Current nutraceuticals in the management of osteoarthritis: a review. *Ther. Adv. Musculoskelet. Dis.* 2012;4:181-207.
19. Percope de Andrade M.A., Campos T.V., Abreu-E-Silva G.M. Supplementary methods in the nonsurgical treatment of osteoarthritis. *Arthroscopy*. 2015;31(4):785–792.
20. Yang S., Eaton C.B., McAlindon T.E., Lapane K.L. Effects of glucosamine and chondroitin supplementation on knee osteoarthritis: an analysis with marginal structural models. *Arthritis Rheumatol*. 2015;67(3):714–723.
21. Akhtar N., Khan N.M., Ashruf O.S., Haqqi T.M. Inhibition of cartilage degradation and suppression of PGE_2 and MMPs expression by pomegranate fruit extract in a model of posttraumatic osteoarthritis. *Nutrition.* 2017;33:1–13.
22. Moon S.M., Lee S.A., Han S.H., Park B.R., Choi M.S., Kim J.S., Kim S.G., Kim, H.J. Chun H.S., Kim D.K., Kim C.S. Aqueous extract of *Codium fragile* alleviates osteoarthritis through the MAPK/NF-κB pathways in IL-1β -induced rat primary chondrocytes and a rat osteoarthritis model. *Biomed. Pharmacother*. 2017;97:264–270.
23. Musumeci G., Trovato F.M., Pichler K., Weinberg A.M., Loreto C., Castrogiovanni P. Extra-virgin olive oil diet and mild physical activity prevent cartilage degeneration in an osteoarthritis model: an in vivo and in vitro study on lubricin expression. *J. Nutr. Biochem*. 2013;24:2064-2075.
24. Musumeci G., Trovato F.M., Imbesi R., Castrogiovanni P. Effects of dietary extra-virgin olive oil on oxidative stress resulting from exhaustive exercise in rat skeletal muscle: A morphological study. *Acta Histochem*. 2014;116:61-69.
25. Khaled M., Jiang Z.Z., Zhang L.Y. Deoxypodophyllotoxin: A promising therapeutic agent from herbal medicine. *J. Ethnopharmacol.* 2013;149(1):24-34.

26. Olaru O.T., Nitulescu G.M., Ortan A., Dinu-Pirvu C.E. Ethnomedicinal, Phytochemical and Pharmacological profile of *Anthriscus sylvestris* as an alternative source for anticancer lignans. *Molecules.* 2015;20(8):15003-15022.
27. Kozawa M., Baba K., Matsuyama Y., Kido T., Sakai M., Takemoto T. Components of the root of *Anthriscus sylvestris* Hoffm. Ⅱ. Insecticidal activity. *Chem. Pharm. Bull(Tokyo)*. 1982;30:2885-2888.
28. Allen D.E., Hatfield G. Medicinal Plants in Folk Tradition: An Ethnobotany of Britain and Ireland. Timber Press. Cambridge. UK. 2004;p.182-183.
29. Wahida B., Amor M., Nabil C. An Inventory of ethnomedicinal plants used in Tunisia. In: Ethnomedicinal Plants: Revitalization of Traditional Knowledge of Herbs. CRC Press. Boca Raton. FL. USA. 2011;p336.
30. Gairola S., Sharma J., Bedi Y.S. A cross-cultural analysis of Jammu, Kashmir and Ladakh (India) medicinal plant use. *J. Ethnopharmacol*. 2014;155(2):925–986.
31. Milovanovic M., Picuric-Jovanovic K., Vucelic-Radovic B., Vrbaski Z. Antioxidant effects of flavonoids of *Anthriscus sylvestris* in Lard. *J. Am. Oil. Chem. Soc.* 1996;73(6):773–776.
32. Dall'Acqua S., Giorgetti M., Cervellati R., Innocenti G. Deoxypodophyllotoxin content and antioxidant activity of aerial parts of *Anthriscus sylvestris* Hoffm. *Z. Naturforsch. C.* 2006;61(9-10):658–662.
33. National Research Council. Guide for the care and use of laboratory animals. eight ad., National Academies Press, Washington, D.C., 2011.
34. Akinnawo O.O., Anyasor G.N., Osilesi O. Aqueous fraction of *Alstonia boonei* de Wild leaves suppressed inflammatory responses in carrageenan and formaldehyde induced arthritic rats. *Biomed Pharmacother* 2017;86:95–101.
35. Glasson S.S., Blanchet T.J., Morris EA. The surgical destabilization of the medial meniscus (DMM) model of osteoarthritis in the 129/SvEv mouse. *Osteoarthr. Cartil*. 2007;15(9):1061–1069.
36. Pritzker K.P., Gay S., Jimenez S.A., Osterqaad K., Pelletier J.P., Revell P.A.,

Salter D., van den Berg W.B. Osteoarthritis cartilage histopathology: grading and staging. *Osteoarthr. Cartil.* 2006;14(1):13-29 .

37. Gilmore T.D. Introduction to NF-κB: players, pathways, perspectives. *Oncogene.* 2006;25:6680-6684
38. Zhou H.Y., Shin E.M., Guo L.Y., Youn U.J, Bae K., Kang S.S., Zou L.B. Kim Y.S. Anti-inflammatory activity of 4-methoxyhonokiol is a function of the inhibition of iNOS and COX-2 expression in RAW 264.7 macrophages via NF-κB, JNK and p38 MAPK inactivation. *Eur. J. Pharmacol.* 2008;586(1-3):340–349.
39. Wang Y.R., Xu Y., Jiang Z.Z., Guerram M., Wang B., Zhu X., Zhang L.Y. Deoxypodophyllotoxin induces G2/M cell cycle arrest and apoptosis in SGC-7901 Cells and inhibits tumor growth *in vivo*. *Molecules.* 2015;20:1661-1675.
40 Khajuria V. Gupta S., Sharma N., Kumar A., Lone N.A. Khullar M., Dutt P., Sharma P.R., Bhaqat A., Ahmed Z. Anti-inflammatory potential of hentriacontane in LPS stimulated RAW264.7 cells and mice model. *Biomed. Pharmacother*. 2017;92:175-186.
41. Yoshimura A. Signal transduction of inflammatory cytokines and tumor development. *Cancer Sci*, 2006;97:439-447.
42. Kim E.Y., Moudgil K.D. Regulation of autoimmune inflammation by pro-inflammatory cytokines. *Immunol. Lett.* 2008;120(1-2):1-5.
43. Lin T.H., Tamaki Y., Pajarinen J., Waters H.A. Woo D.K. Yao Z., Goodman SB. Chronic inflammation in biomaterial induced periprosthetic osteolysis: NF-κB as a therapeutic target. *Acta. biomaterialia.* 2014;10(1)1-10.
44. Surh Y.J., Chun K.S., Cha H.H., Han S.S., Keum Y.S., Park K.K, Lee S.S. Molecular mechanism underlying chemopreventive activities of anti-inflammatory phytochemicals: down-regulation of COX-2 and iNOS through suppression of NF-kappa B activation. *Mutat. Res.* 2001;1(480-481):243-268.

45. Liu Y., Fang S., Li X., Feng J., Du J., Guo L., Su Y., Zhou J., Ding G., Bai Y., Wang S., Wang H., Lit Y. Aspirin inhibits LPS-induced macrophage activation via the NF-κB pathway. *Sci. Rep*. 2017;7(1):11549.
46. Kim K.N., Heo S.J., Yoon W.J., Kang S.M., Ahn G., Yi T.H., Jeon Y.J. Fucoxanthin inhibits the inflammatory response by suppressing the activation of NF-κB and MAPKs in lipopolysaccharide-induced RAW264.7 macrophages. *Eur. J. Pharmacol*. 2010;649(1-3):369-375.
47. Niu X., Li Y., Li W., Hu H., Yao H., Li H., Mu Q. The anti-inflammatory effects of *Caragana tangutica* ethyl acetate extract. *J. Ethnopharmacol*. 2014;152(1):99-105.
48. Cao L., Li R., Chen X., Xue Y., Liu D. Neougonin A inhibits lipopolysaccharide-induced inflammatory responses via downregulation of the NF-κB signaling pathways in RAW264.7 macrophages. *Inflammation*. 2016;39(6):1939-1948.
49. Sung J., Jeon H., Kim I.H., Jeong H.S., Lee J. Anti-inflammatory effects of stearidonic acid mediated by suppression of NF-κB and MAP-kinase pathways in macrophages. *Lipids*. 2017;52(9):781-787.
50. Gao X., Lin X., Li X., Zhang Y., Chen Z., Li B. Cellular antioxidant, methylglyoxal trapping, and anti-inflammatory activities of cocoa tea (*Camellia ptilophylla* Chang). *Food Funct.* 2017;1:2836-2846.
51. Jaja-Chimedza A., Graf B.L., Simmler C., Kim Y., Kuhn P., Pauli G.F., Raskin I. Biochemical characterization and anti-inflammatory properties of an isothiocyanate-enriched moringa (*Moringa oleifera*) seed extract. *PLoS One*. 2017;12(8):e0182658.
52. Yang J.H., Choi M.H., Yang S.H., Cho S.S., Park S.J. Shin H.J. Ki S.H. Potent anti-inflammatory and antiadipogenic properties of Bamboo (*Sasa coreana* Nakai) leaves extract and its major constituent flavonoids. *J. Agric. Food Chem*. 2017;65(31):6665-6673.
53. Crunkhorn P., Meacock S.C. Mediators of the inflammation induced in the

rat paw by carrageenan. *Br. J. Pharmacol.* 1971;42(3):392-402.

54. Vinegar R., Schreiber W., Hugo R. Biphasic development of carrageenan edema in rats. *J. Pharmacol. Exp. Ther.* 1969;166(1):96–103.
55. Chaudhari S.S., Chaudhari S.R., Chavan M.J. Analgesic, anti-inflammatory and anti-arthritic activity of *Cassia uniflora* Mill. *Asian Pac. J. Trop. Biomed.* 2012;2:181–186.
56. Felson D.T., Lawrence R.C., Hochberg M.C., McAlindon T., Dieppe P.A., Minor M.A., Blair S.N., Berman B.M., Fries J.F., Weinberger M., Lorig K.R., Jacobs J.J., Goldberg V. Osteoarthritis: new insights. Part 2: treatment approaches. *Ann. Intern. Med.* 2000;133(9):726–737.
57. Musumeci G., Castrogiovanni P., Trovato F.M., Weinherg A.M., Al-Wasiyah M.K., Alqahtani M.H., Mobasheri A. Biomarkers of chondrocytes apoptosis and autophagy in osteoarthritis. *Int. J. Mol. Sci.* 2015;16(9):20560-20575.
58. Tortorella M.D., Burn T.C., Pratta M.A., Abbaszade I., Hollis J.M., Lui R., Rosenfeld S.A., Copeland R.A., Decicco C.P., Wynn R., Rockwell A., Yang F., Duke J.L., Solomon K., George H., Bruckner R., Nagase H., Itoh Y., Ellis D.M., Ross H., Wiswall B.H., Murphy K., Hillman Jr M.C., Hollis G.F., Newton R.C., Magolda R.L., Trzaskos J.M., Arner E.C. Purification and cloning of aggrecanase-1: a member of the ADAMTS family of proteins. *Science*. 1999;284(5420):1664–1666.
59. Ahmed S., Wang N., Hafeez B.B., Cheruvu V.K., Haqqi T.M. *Punica granatum* L. extract inhibits IL-1beta-induced expression of matrix metalloproteinases by inhibiting the activation of MAP kinases and NF-kappaB in human chondrocytes *in vitro*. *J. Nutr*. 2005;135(9):2096–2102.
60. Shiozawa S., Shimizu K., Tanaka K., Hino K. Studies on the contribution of c-fos/AP-1 to arthritic joint destruction. *J. Clin. Invest.* 1997;99(6):1210–1216.
61. Firestein G.S., Manning A.M. Signal transduction and transcription factors in rheumatic disease. *Arthritis Rheum*. 1999;42(4):609–621.
62. Iijima H., Aoyama T., Ito A., Tajino J., Nagai M., Zhang X., Yamaguchi S.,

Akiyama H., Kuroki H. Destabilization of the medial meniscus leads to subchondral bone defects and site-specific cartilage degeneration in an experimental rat model. *Osteoarthr. Cartil*. 2014;22(7):1036-1043.

63. Musumeci G., Castrogiovanni P., Mazzone V., Szychlinska M.A., Castorina S., Loreto C. Histochemistry as a unique approach for investigating normal and osteoarthritic cartilage. *Eur. J. Histochem.* 2014;58(2):2371.
64. Žemlička L., Fodran P., Lukeš V., Vagánek A., Slováková M., Staško A., Dubaj T., Liptaj T., Karabín M., Birošová L., Rapta P. Physicochemical and biological properties of luteolin-7-O-β-D-glucoside (cynaroside) isolated from *Anthriscus sylvestris* (L.) Hoffm. *Monatsh. Chem. Chem. Mon*. 2014;145(8):1307−1318.
65. Feng Y., Yu Y.H., Wang S.T., Ren J., Camer D., Hua Y.Z. Zhang Q., Huang J., Xue D.L., Zhang X.F., Huang X.F., Liu Y. Chlorogenic acid protects d-galactose-induced liver and kidney injury via antioxidation and antiinflammation effects in mice. *Pharm. Biol.* 2016;54(6):1027-1034.
66. Costa G., Ferreira J.P., Vitorino C., Pina M.E., Sousa J.J., Fiqueiredo I.V., Batista M.T. Polyphenols from *Cymbopogon citratus* leaves as topical anti-inflammatory agents. *J. Ethnopharmacol.* 2016;3(178):222-228.

감사의 글

박사학위를 준비했던 지난 3년간은 저에게 있어 지식의 가치와 배움의 기쁨을 알게 해준 너무나도 소중한 시간이었습니다. 석사 졸업하고 나태해질대로 나태해진 내 삶에 학문에 대한 열정을 다시 심어주신 저의 지도교수님, 김춘성 교수님과 그 길을 독려해주시고 존재 자체만으로도 항상 큰 힘이 되어주신 김도경 교수님께 큰 절을 올립니다. '대학원이란 선생이 학생에게 학문을 가르칠 뿐만 아니라 학생이 선생의 등을 보면서 인생의 삶을 배우는 것이다'라고 말한 누군가의 말처럼 거칠게 없었던 저를 항상 존중으로 대해주시고 사랑으로 지켜주신 두 교수님에게서 학문 이상으로 인생에 대한 자세를 배웠습니다. 비록 그런 큰 사람이 되기에는 아직 갈 길이 멀지만 항상 마음깊이 간직하고 닮아가도록 노력하겠습니다. 두 분의 넘치는 사랑에 감사드립니다.

언제나 후배들에게 많은 걸 알려주고 싶어 하시고 동기부여를 해주셨던 열정이 넘치신 김재성 교수님, 논문 쓰는 법, 실험하는 법, 연구계획서 쓰는 법 등 석사 때부터 지금까지 많은 걸 교수님께 배웠고, 제가 지금까지 이루어 낸 업적들 중 어느 것 하나 교수님 손을 거치지 않은 것이 없습니다. 비록 다른 연구실이여도 커피 가질러 오시면서 짧은 시간이라도 discussion해주시고 관심있게 지도해주셔서 감사합니다. 그리고 씨에스텍 연구소장 겸 우리 연구실에서 교수님 다음으로 수장이신 문성민 박사님, 말 안 듣는 저 때문에 많이 속상해 하시고 힘들어 하셨지만 연구의 목표 달성을 위해 실험 과정 과정들을 자세히 설명해주시고 알려주셔서 감사합니다. 비록 지금은 다른 자리로 가셨지만 한 곳에만 있음으로 실험 방법의 다양성을 잘 알지 못했던 저에게 많은 노하우와 팁을 알려주셨던 황은주 선생님, 선생님의 깨끗하고 군더더기 없는 실험 결과와 여의치 않는 상황임에도 주말에도 나와서 논문 찾던 모습이 아직도 머릿속에 생생합니다. 덕분에 제가 분발할 수 있었습니다. 석사 때부터 같이 동고동락했던 보람언니, 같이 지낸 오랜 세월만큼 언니와 쌓은 많은 추억들이 새록새록 떠오릅니다. 덕분에 참 즐거웠고 의지도 많이 했습니다. 지금까지 고생한만큼 하루 빨리 좋은 결실 맺기를 기도합니다. 그리고 우리 방 꼬맹이 둘, 더 많은 실험을 배우고 싶다고 그 좋은

직장을 그만두고 열정을 뿜내고 있는 미림이와 반전매력 우리 방 꼬맹이 지연이, 모두 내가 잘 못 챙겨줬음에도 불구하고 항상 웃으며 잘 따라줘서 고맙고 오히려 많이 챙김을 받아서 정말 고마워.

마지막으로 여리디 여린 우리 엄마, 부모의 한없는 사랑을 가장 잘 보여주시고 그 모든 일에 항상 제가 먼저이셨던 그 무한한 사랑에 대한 감사를 어떻게 다 할 수 있을까요. 비록 처음에는 박사학위 시작을 반대하셨지만 막상 힘들 때 가장 많이 위로해주시고 내 편이 되어주시며 같이 힘들어해주셨던 우리 엄마. 그저 죄송하고 감사합니다. 그리고 사랑합니다.

학위 심사를 위해 멀리서 오신 숙명여대 양 영 교수님과 석사 때부터 지금까지 항상 웃는 얼굴로 맞아주시고 저의 학위 심사 위원장이신 김흥중 교수님께도 감사 인사를 드립니다. 다 언급하진 못하였지만, 이 외 제가 학위하는 과정동안 많은 도움을 주신 모든 선생님들, 그리고 교수님들께 감사 인사를 드립니다. 이제 다시 시작의 기로에 서 있습니다. 많은 것을 받고 얻은 만큼 이것을 양분삼아 좋은 연구를 통해 보답하도록 하겠습니다. 감사합니다.

2018년 마지막 달에 이슬아